Chem Soc Rev

Quantum Dynamics of Polyatomic Dissociative Chemisorption on Transition Metal Surfaces: Mode Specificity and Bond Selectivity

Journal:	*Chemical Society Reviews*
Manuscript ID:	CS-REV-05-2015-000360.R1
Article Type:	Review Article
Date Submitted by the Author:	05-Jun-2015
Complete List of Authors:	jiang, bin; University of New Mexico, Chemistry and Chemical Biology Yang, Ming-Hui; Wuhan Institute of Physics and Mathematics of the Chinese Academy of Sciences, Xie, Daiqian; Nanjing University, Department of Chemistry Guo, Hua; University of New Mexico, Department of Chemistry

Quantum Dynamics of Polyatomic Dissociative Chemisorption on Transition Metal Surfaces: Mode Specificity and Bond Selectivity

*Bin Jiang,[1,2] Minghui Yang,[3] Daiqian Xie,[4,5] and Hua Guo[1,]**

[1]*Department of Chemistry and Chemical Biology, University of New Mexico, Albuquerque, New Mexico, 87131, USA*

[2]*Department of Chemical Physics, University of Science and Technology of China, Hefei 230026, China*

[3]*Key Laboratory of Magnetic Resonance in Biological Systems, State Key Laboratory of Magnetic Resonance and Atomic and Molecular Physics, Wuhan Centre for Magnetic Resonance, Wuhan Institute of Physics and Mathematics, Chinese Academy of Sciences, Wuhan 430071, China*

[4]*Institute of Theoretical and Computational Chemistry, Key Laboratory of Mesoscopic Chemistry, School of Chemistry and Chemical Engineering, Nanjing University, Nanjing 210093, China*

[5]*Synergetic Innovation Center of Quantum Information and Quantum Physics, University of Science and Technology of China, Hefei, Anhui 230026, China*

*: Corresponding author, hguo@unm.edu

Abstract

Dissociative chemisorption is the initial and often rate-limiting step in many heterogeneous processes. As a result, an in-depth understanding of the reaction dynamics of such processes is of great importance for the establishment of a predictive model of heterogeneous catalysis. Overwhelming experimental evidence has suggested that these processes have a non-statistical nature and excitations in various reactant modes have a significant impact on reactivity. A comprehensive characterization of the reaction dynamics requires a quantum mechanical treatment on a global potential energy surface. In this review, we summarize recent progress in constructing high-dimensional potential energy surfaces for polyatomic molecules interacting with transition metal surfaces based on plane-wave density functional theory and in quantum dynamical studies of dissociative chemisorption on these potential energy surfaces. A special focus is placed on the mode specificity and bond selectivity in these gas-surface collisional processes, and their rationalization in terms of the recently proposed Sudden Vector Projection model.

I. Introduction

The interaction of gas phase molecules with metal surfaces is an important area of current research.[1] Such interaction might result in diffraction, scattering, adsorption, dissociation, and reactions of the molecules.[2] This review is concerned with the dissociative chemisorption (DC), in which a gas phase molecule dissociates upon collision with a surface, leading to chemisorbed products. It is well established that DC is the necessary first step in many heterogeneous catalytic processes such as ammonia synthesis, steam reforming, and water-gas shift (WGS) reaction, etc.[3] In many such reactions, DC is also the rate-limiting step. For example, the Bosch-Haber process for producing ammonia is initiated by the DC of both H_2 and N_2 and limited by the latter.[4] Similarly, the DC of water is the initial and rate-limiting step of the WGS reaction at low temperatures.[5] Furthermore, the major industrial process for hydrogen production, namely the steam reforming of natural gas (CH_4) to syngas (H_2 + CO), is limited by the DC of CH_4.[6] Syngas is in turn an important feedstock for other catalytic processes such as the Fischer-Tropsch synthesis for producing higher hydrocarbons. As a result, it is of great importance to understand the DC dynamics if predictive models of catalysis and other heterogeneous processes are to be developed.

With few exceptions,[7] DC processes are activated, because they involve the cleavage of a bond in the molecule. As a result, energy is required to overcome the barrier in such reactive events. While thermal activation is often effective, as in many industrial settings, it does not provide sufficient information on the effectiveness of various reactant degrees of freedom in promoting the reaction. Detailed information with reactant quantum state resolution is needed to understand the influence of reactant modes on the reactivity, particularly in comparison with the translational motion. This so-called mode specificity is of central importance in understanding

the dynamics of chemical reactions both in the gas phase and at gas-surface interfaces.[8-13] With the advent of laser and molecular beam techniques, gas-surface collisional dynamics can now be investigated experimentally in high vacuum with a quantum state resolution.[9,14-19] Such experimental studies shed valuable light on the reaction dynamics of DC processes.

DC of diatomic molecules such as H_2 is now well understood and the reader is referred to several excellent reviews on this topic.[7,20-23] The existence of a single vibrational degree of freedom in these cases renders its mode specificity relatively straightforward to understand. We focus here on the DC of polyatomic molecules, where the multiple vibrational modes not only offer much richer mode specificity but also pose a greater challenge.[24-25] In particular, the DC of methane (CH_4) and its isotopomers has severed as an important proving ground for polyatomic reaction dynamics on transition metal surfaces.[9,18] Recent molecular beam studies, mostly in the laboratories of Beck and Utz, have demonstrated strong mode specificity in this process.[26-45] In Figure 1, the initial sticking probabilities (S_0) of methane on Ni(100) in various vibrational states are shown as a function of the translational energy in the direction of the surface normal (E_t). It is readily seen that the DC of methane is activated by translational energy as S_0 increases rapidly with the increasing E_t. In addition, this process is also promoted by vibrational excitations, as shown by the horizontal shifts of the S_0 curves for vibrationally excited methane. For example, the DC of methane in its first excited state of the symmetric stretching mode (v_1=1) was found to be the most effective, more than the translational mode excited with the same amount of energy.[34] This is followed by the antisymmetric stretching mode fundamental (v_3=1), which is about as effective as the same amount of translational energy.[26] The least effective is the umbrella bending mode (v_4=1).[33] The relative efficacy between the vibrational and translational excitations can be quantified by the so-called vibrational efficacy:[46]

$$\eta = \frac{E(0, S_0) - E(v, S_0)}{\Delta E_v}, \quad (1)$$

where the numerator is the translational energy gap between the reaction curves for the ground (0) and excited (v) vibrational levels of the molecule and ΔE_v the energy difference between the vibrational levels. Thus, an η value larger than 1.0 would indicate that the vibrational energy is more effective than translational energy in promoting the reaction, and *vice versa*. In Table I, the experimentally measured vibrational efficacies of various vibrational modes of CH_4 on a number of transition metal surfaces are shown. Note that the experimental data were usually fit to the *S*-shaped reactivity curves suggested by Luntz,[46] resulting in vibrational efficacies that are independent of translational energy. However, this is not necessarily always true as shown in recent theoretical calculations (*vide infra*). Consequently, the vibrational efficacy is better given within a range. The apparent mode specificity underscores the fact that all forms of energy are not equal in promoting this gas-surface reaction, and argues against a statistical treatment which assumes no distinction among energies in different forms. Indeed, the existence of mode specificity suggests the importance of dynamics.[8,10]

A related phenomenon is the so-called bond selectivity. The issue at hand is the efficacy for breaking a specific bond *via* vibrational excitation of the reactant.[47] For the methane DC, experimental data have shown that the excitation of the local C-H vibration in CHD_3 greatly promotes its cleavage on Ni(111).[36] More recent experimental studies have examined the bond selective chemistry involving CHD_3, CH_2D_2, and CH_3D on Pt(111).[42] Like mode specificity, bond selectivity is also an important manifestation of dynamics.[47]

More recently, the mode specificity in the DC of water, which is of fundamental importance in steam reforming and the WGS reaction, was examined experimentally on Ni(111).[48] The findings indicated that the excitation of the antisymmetric stretching mode of D_2O greatly enhances the reactivity, more than the same energy in the translational mode. This observation suggests that mode specific DC reactions are not restricted to methane.

The pioneering experimental studies mentioned above demand in-depth theoretical insights. They also provide stringent tests for theoretical models. To properly treat the non-statistical DC processes involving polyatomic molecules, dynamical models are necessary,[25,49-50] in which global potential energy surfaces (PESs) are explicitly or implicitly required. Despite tremendous progress in plane-wave density functional theory (DFT) in treating surface problems,[51] the development of such PESs for DC of polyatomic molecules remains quite challenging as a high-dimensional analytic representation of a large number of DFT points in a vast configuration space relevant to the reaction is needed. Apart from high fidelity, an analytical representation of the PES should also be easy to evaluate and satisfy symmetry requirements, which include both the translational periodicity of the surface and permutation symmetry of the molecular system. Indeed, the accurate and efficient representation of the global PES poses the first challenge for first-principles characterization of the DC dynamics.

In passing, we note that *ab initio* molecular dynamics (AIMD) calculations, in which the forces acting on the system are calculated on the fly by solving the electronic Schrödinger equation, have recently been applied to study DC dynamics.[52-56] While providing valuable information on the dynamics, nevertheless, AIMD calculations are still too expensive to predict initial sticking probabilities in the experimental energy range for reactions considered here. They

neglect important quantum effects as well. As a result, they will not be discussed here in detail, except in comparison with results obtained by other means.

The availability of such global PESs facilitates both quasi-classical trajectory (QCT) and quantum dynamical (QD) calculations of the dissociation dynamics. Although the former is much less expensive and sheds valuable light on the reaction dynamics, we argue that a QD treatment is preferred because of potentially important quantum effects such as tunneling and zero-point energy. After all, the DC of a molecule such as methane or water involves the transfer of a light atom (H) over a substantial barrier. While the QD calculations are quite intensive, they produce the most reliable results to compare with experiment. Thus, the QD characterization of DC processes of polyatomic molecules constitutes the second challenge for *ab initio* simulations of DC dynamics.

In recent years, much progress has been made to meet both challenges. The advances significantly improved our understanding DC dynamics of polyatomic molecules and molecule-surface interaction in general. In this review, we discuss the recent advances in both the construction of high-dimensional PESs and QD studies on these PESs, focusing on the DC of methane and water on various transition metal surfaces. Our review will also attempt to unravel the underlying physics in the observed mode specificity and bond selectivity in DC reactions. To this end, we introduced a transition-state based model for predicting the relative efficacies of various reactant modes.[57-59] This so-called Sudden Vector Projection (SVP) model rationalizes these non-statistical phenomena in terms of the couplings of various reactant modes with the reaction coordinate at the transition state, which can be approximated by the projection of the reactant normal mode vectors onto the reaction coordinate vector. The SVP model provides a useful framework for understanding the observed mode specificity and bond selectivity in DC

processes. This review is organized as follows. The next section (Sec. II) discusses the challenges in constructing high-dimensional global PESs for DC processes and recent developments. Section III outlines various QD approaches to characterize the reaction dynamics on the high-dimensional PESs. The SVP model is briefly reviewed in Sec. IV. In Sec. V, our current understanding of the DC dynamics of both methane and water is presented. Finally, conclusions and prospects are given in Sec. VI.

II. Potential Energy Surfaces

We will focus here on the adiabatic regime, in which the collision of a molecule with a metal surface does not involve electron-hole (e-h) pairs of the metal, which are quite prevalent in surface photochemistry.[60-61] In scattering systems, this is a reasonable approximation for the systems discussed in this review, as the e-h pair involvement is often associated with for molecules with large electron affinities, such as NO.[17,19] Kroes and coworkers have recently presented evidence that e-h pairs play a minor part in the DC of H_2 on Pt(111).[62] Similar conclusion has also been reached by others for the DC of H_2 on Cu(110) and of N_2 on W(110).[63] A more recent experiment of Beck and coworkers found little evidence of hot electrons or holes in the DC of vibrationally excited CH_4 on Pt(111).[45] This lack of strong interaction with the substrate e-h pairs can presumably be rationalized by the high-energy LUMO (lowest unoccupied molecular orbital) in these species.

Furthermore, we assume that the solid surface is rigid in our QD models. This is a much weaker assumption as the energy transfer between the impinging polyatomic molecule and surface, which depends on the ratio of molecular and surface effective masses according to the simple Baule model,[64] will almost certainly take place. In addition, the motion of surface atoms

may also influence the energetics and dynamics of the scattering process. Unfortunately, a fully quantum dynamical treatment of all relevant surface atoms is still impractical. Instead, in our theoretical treatments, these lattice effects are corrected using several well-tested models, as discussed extensively by Jackson and coworkers.[49-50] Some of the key points of these models will be discussed in more detail below.

Under this so-called Born-Oppenheimer static surface (BOSS) approximation,[21] the number of degrees of freedom for an *N*-atom molecule is reduced to a manageable number (3*N*). Nevertheless, the dimensionality is still very high and many DFT calculations have to be performed at geometries spanning a large configuration space relevant to the reaction. To facilitate dynamical calculations, these DFT points need be represented by an analytical function that is faithful and efficient to evaluate. In addition, the PES should be invariant with respect to the permutation of identical atoms in the molecule although the exchange of identical surface atoms can be ignored due to the static nature of the model. Furthermore, such a PES should also satisfy the periodicity of the surface.[65] These characteristics of the PES are of paramount importance in dynamics studies, since incorrect or inaccurate PESs cannot be expected to yield correct dynamical information no matter how accurate the dynamical method might be.

The early modified London-Eyring-Polanyi-Sato (LEPS) PES proposed by McCreedy and Wolken for H_2 dissociation on W(001) fulfills these symmetry requirements,[66] but it only applies to diatom-surface systems and its analytic form is not sufficiently flexible. In 2000, Busnengo *et al*. introduced a corrugation reducing procedure (CRP) to represent diatom-surface PESs.[67] This interpolation-based method is accurate and accounts for symmetry using Jacobi coordinates, but its extension to polyatomic systems is not straightforward.[68] Later, Kroes and coworkers adapted the modified Shepard interpolation (MSI) scheme of Collins[69-70] as a general

solution for constructing PESs of molecule-surface systems.[71] Permutation symmetry is enforced by including permutationally equivalent molecular configurations in the data set, thus with larger computational costs. The surface symmetry is only enforced approximately by translation or reflection when the center of mass (COM) of the molecule is outside the unit cell, which may cause discontinuities in the derivatives of the PES at boundaries.[72] Frankcombe *et al*. recently solved this problem by introducing redundant coordinates that explicitly take into account the surface periodicity.[73] However, MSI is rather slow for high-dimensional problems due to its interpolation nature and the PES can be quite bumpy if an insufficient number of points is included.

An alternative and general approach is the permutation invariant polynomial (PIP) method, which was initially developed by Bowman and coworkers for gas phase PESs.[74-75] Using a PIP representation, the PES is expanded in terms of symmetrized monomials:[76]

$$V = \sum_l c_l \hat{S} P_l = \sum_l c_l \hat{S} \prod_{i<j}^{N} p_{ij}^{l_{ij}}, \qquad (2)$$

where N is the number of atoms in the molecule. $p_{ij} = \exp(-\alpha r_{ij})$ are the Morse-like variables with α as a length parameter and r_{ij} the $N(N\text{-}1)/2$ internuclear distances.[74] l_{ij} is the degree of p_{ij} and $l = \sum_{i<j}^{N} l_{ij}$ is the total degree in each monomial. $\hat{S}$ is the symmetrization operator for the permutation symmetry in the system. The fitting is performed by a linear least squares method, which is very efficient and robust. Thanks to the polynomial form, the evaluation of the PES is also inexpensive. This approach has been widely used in gas-phase systems, the reader is referred to excellent reviews on the details of the PIP method and applications.[74-75] We have

recently extended this approach to polyatomic molecule-surface systems, albeit in reduced dimensionality in which the surface is assumed to be a "pseudo" sphere.[48,77-78] It turns out that the linear expansion of the PES in terms of the PIPs may not be sufficiently flexible for complex molecule-surface reactions, leading to somewhat large fitting errors. Also, one has to treat the surface periodicity approximately as in the MSI method.

Another promising approach for fitting high-dimensional molecule-surface PESs is the neural network (NN) method. NNs provide an extremely flexible non-linear fitting formalism that is capable of producing a very accurate representation of a large number of *ab initio* points. This approach has been gaining popularity in both gas-phase and surface problems.[79-81] Indeed, several NN based PESs have been reported for molecule-surface interactions.[82-87] Importantly, attention has been paid to the adaptation of both surface periodicity and permutation invariance. For example, Lorenz *et al.* proposed a set of symmetry-adapted coordinates specific for hydrogen DC on Pd(100).[82-83] However, their approach is difficult to extend to polyatomic molecules. Ludwig and Vlachos combined CRP and NN fitting, in which the surface periodicity was considered in Fourier expansions of atomic lateral coordinates.[85] Behler and coworkers[84] devised a similar symmetry adaptation scheme using Fourier expansions of the distances between each atom and high symmetry sites on the surface. Although these methods have been tested for DC of diatomic molecules and are in principle applicable for different surface types and molecular sizes, the permutation invariance is only approximately adapted by either duplicating the data where identical atoms are exchanged or incomplete symmetrization of the Fourier terms. This issue in fact becomes more complicated for DC of polyatomic molecules.

Very recently, we proposed a new, simple, general, and rigorous way to impose both the translational and permutation symmetries.[88] Our method is an extension of the permutation

invariant polynomial-neural network (PIP-NN) method recently proposed by us for PESs of isolated species,[89-90] which has been successfully applied to several polyatomic systems up to twelve dimensions.[91-94] The PIP-NN method uses PIPs of primitive coordinate functions as symmetry functions in the input layer of the NN, thus guaranteeing the permutation invariance of the PES. For surface problems, the primitive functions are replaced by ones that contain the surface periodicity. Taking the example of a homonuclear diatom on the (111) surface of a metal, one can define the primitive functions as follows:[85]

$$G_i = \cos(\frac{4\pi Y_i}{a\sqrt{3}}) + 2\cos(\frac{2\pi X_i}{a})\cos(\frac{2\pi Y_i}{a\sqrt{3}}), \quad (3)$$

$$G_{i+3} = \sin(\frac{4\pi Y_i}{a\sqrt{3}}) - 2\cos(\frac{2\pi X_i}{a})\sin(\frac{2\pi Y_i}{a\sqrt{3}}), \quad (4)$$

$$G_{i+6} = \exp(-\lambda Z_i), \quad (5)$$

$$G_{10} = \exp(-\lambda r), \quad (6)$$

where r the internuclear distance in the molecule and X_i, Y_i, Z_i are the Cartesian coordinates with i denoting the atoms (=1,2) and COM (=3), respectively; and. Here, a is the unit cell length and λ is a parameter. The terms in Eqs. (3-4) are essentially the same as these proposed by others,[85,95] enforcing the surface periodicity. One can further improve the flatness of the asymptotic potential with respect to lateral coordinates at large Z values by including the exponential Z-dependent terms in Eq. (5) in Eqs. (3-4).[96]

To adapt the permutation symmetry, the following low-order PIPs of the primitive functions are used as the input layer of an NN:[88]

$$G_1' = G_1+G_2\,,\; G_2' = G_4+G_5\,,\; G_3' = G_7+G_8 \tag{7}$$

$$G_1'' = G_1G_2\,,\; G_2'' = G_4G_5\,,\; G_3'' = G_7G_8\,, \tag{8}$$

$$G_1'''= G_1G_4+G_2G_5\,,\; G_2''' = G_1G_7+G_2G_8\,,\; G_3'''= G_4G_7+G_5G_8 \tag{9}$$

along with the G_{i+6} and G_{10} terms. It was pointed out[88] that the cross terms such as those in Eq. (9) are essential to avoid unphysical symmetries associated with the exchange of individual atomic coordinates, which are presumably the culprit for the poor performance of the previous symmetrization schemes.[84,86] Our PIP-NN scheme is shown in diatomic DC to produce at least an order of magnitude smaller fitting errors than previous schemes,[88] thanks to elimination of the over-symmetrization. In other words, the PIP-NN method recognizes the importance of involving the correct rather than "intuitive" but non-existing permutation symmetry.

The most distinct feature of the PIP-NN approach is that it can be easily generalized to polyatomic molecule-surface systems, simply by increasing the number of the primitive functions for atoms, and imposing permutation symmetry by using low-order PIPs generated using symmetrization operators.[74,76] For systems with a large number of identical atoms, such as CH_4 which has 4!=24 permutations, the number of DFT points can be significantly reduced thanks to the permutation symmetry. We also note that no modification of the NN is needed and the PIP-NN PES is very efficient to evaluate, much more so than interpolation-based methods such as MSI. Finally, the flexibility of the NNs allows a high-fidelity fitting of the PES, with small average errors. This approach has recently been used in the successful construction of the water-Ni(111) PES in its full nine dimensions.[96]

As mentioned above, the electronic structure of gas-surface systems has in most studies been treated within the DFT framework. Since the plane-wave DFT method has been extensively discussed in the literature,[51] only a brief discussion is given here. In these calculations, the metal surface is represented by a multilayer slab that is periodic in the *X* and *Y* directions and separated in the *Z* direction by a large vacuum. While the wave function of the valence electrons is expanded in terms of plane wave bases with a large cutoff energy, the core electrons are approximated using the projector augmented-wave (PAW) method.[97] The size of the unit cell is often determined such that the interaction between adjacent molecules is negligible. The Brillouin zone is sampled with a Monkhorst-Pack *k*-point grid.[98] Functionals with the generalized gradient approximation, such as PBE[99] and PW91,[100] are often used. Spin polarization should be included whenever necessary. At each geometry, the total energy in the limit of zero temperature[101] is used for the construction of the PES. In all our calculations, the Vienna *Ab-initio* Simulation Package (VASP) suite of codes[102-103] was used. It should be noted that the DFT is not a truly *ab initio* method, and the description of the electronic structure is thus approximate in nature, depending for example on the functional used. As a result, it should be kept in mind that significant errors might ensue. There are several more accurate and reliable alternatives to the DFT approach for surface problems, but the computational costs are still very high.[104] Consequently, in many cases comparison with experiment remains the only way to verify the accuracy of the electronic structure calculations.

III. Reaction Dynamics

Once a global PES becomes available, the DC dynamics can be investigated using either a QCT or wave packet based QD method. The former assumes that the nuclear dynamics follows the Newtonian mechanics and is thus considerably less expensive computationally. While the

QCT method approximates the initial internal quantum state of the molecule impinging on the surface, it does not account for other quantum effects such as tunneling and resonances. It might also suffer from the so-called zero-point energy (ZPE) leakage, in which the energy in the internal degrees of freedom of the reactant flows to other degrees of freedom, before reaching the transition state. As a result, the QCT approach is mostly suitable for energies higher than the reaction barrier, and even then, the results should be taken with caution. On the other hand, it can provide useful information on trends and important mechanistic insights. As the QCT method has been discussed extensively in the literature,[105-107] no technical detail of the method is given here. Our QCT calculations were performed using the VENUS program[108] modified by us.

Instead, we will focus here on the time-dependent QD method based on wave packet propagation, which naturally takes into account all quantum effects. This is particularly important as most experiments so far were performed in the tunneling regime. The QD method has been used in studying DC dynamics on diatomic systems with either a time-independent coupled-channel method[7] or a time-dependent wave packet propagation formalism.[21] The latter scales more favorably than its time-independent counterpart for high-dimensional problems, and is thus widely used in dynamical calculations. For polyatomic molecules, the majority of previous models have approximated them as pseudo-diatoms using time-dependent QD method.[109-120] Such drastic simplifications do not do justice to these complex systems. In particular, the symmetric and antisymmetric stretching modes of methane cannot be distinguished in such a simple model. A better understanding of DC dynamics would thus require high-dimensional approaches.

Taking a triatomic molecule such as H_2O in the BOSS approximation as an example, the nine-dimensional (9D) Hamiltonian assumes the following form ($\hbar = 1$ hereafter):

$$\hat{H} = -\frac{1}{2M}\frac{\partial^2}{\partial X^2} - \frac{1}{2M}\frac{\partial^2}{\partial Y^2} - \frac{1}{2M}\frac{\partial^2}{\partial Z^2} - \frac{1}{2\mu_1}\frac{\partial^2}{\partial r_1^2} - \frac{1}{2\mu_2}\frac{\partial^2}{\partial r_2^2} + \frac{\hat{j}^2}{2\mu_1 r_1^2} + \frac{\left(\hat{J}-\hat{j}\right)^2}{2\mu_2 r_2^2} + V\left(X,Y,Z,r_1,r_2,\theta_1,\theta_2,\varphi,\phi\right). \quad (10)$$

As illustrated in Figure 2, *X*, *Y*, *Z* are the Cartesian coordinates for the H_2O COM above the surface, the r_1 is the bond length of non-dissociative OH bond, r_2 the distance between the COM of OH and H. The corresponding masses are defined as follows: $M = m_{H_2O}$, $\mu_1 = m_H m_O/(m_H + m_O)$, $\mu_2 = m_{OH} m_H/(m_{OH} + m_H)$. $\hat{j}$ and $\hat{J}$ are the angular momenta for the OH fragment and H_2O triatom, respectively, and they are defined by the Jacobi angles $(\theta_1, \theta_2, \varphi)$. *V* is the PES.

In our reduced-dimensional model for the DC of H_2O,[77,121-122] the translational degrees of freedom parallel to the surface (*X* and *Y*) are ignored, as they are not considered essential for the reaction. We further assume the surface is flat, and the PES is thus isotropic in ϕ while depending on the other six coordinates.[122] Hence, the dynamics can be approximated by this six-dimensional (6D) model with the following Hamiltonian:[77,121-122]

$$\hat{H} = -\frac{1}{2M}\frac{\partial^2}{\partial Z^2} - \frac{1}{2\mu_1}\frac{\partial^2}{\partial r_1^2} - \frac{1}{2\mu_2}\frac{\partial^2}{\partial r_2^2} + \frac{\hat{j}^2}{2\mu_1 r_1^2} + \frac{\left(\hat{J}-\hat{j}\right)^2}{2\mu_2 r_2^2} + V\left(Z,r_1,r_2,\theta_1,\theta_2,\varphi\right). \quad (11)$$

The Hamiltonian and wave packet can be discretized with a mixed discrete variable representation (DVR) and finite basis representation (FBR).[123] The *Z* and r_2 coordinates were discretized with the sine DVR, while r_1 treated as non-reactive with a potential optimized DVR (PODVR).[123] The overall rotational basis for the H_2O moiety is described by normalized Wigner

function $\bar{D}^{*J}_{MK}(\phi,\theta_2,\varphi)$, which can be expressed as $\sqrt{\frac{2J+1}{8\pi^2}}e^{iM\phi}d^J_{MK}(\theta_2)e^{iK\varphi}$.[124] K and M are the projections of J on the molecule-fixed z-axis which is along r_2 and on the surface normal, respectively. Within the flat surface model where the PES is independent of the azimuthal angle ϕ, M is conserved and as a result this degree of freedom is not explicitly treated in our dynamical model.[122] Nonetheless, the dynamics depends through the Wigner rotational matrix on the quantum number M, which specifies the orientation of the impinging H_2O molecule. In addition to the rotational basis for the triatom, the other rotational/bending degree of freedom is described by the normalized associated Legendre polynomial $\bar{P}^K_j(\cos\theta_1)$.

In the absence of an external field, the molecule above the surface possesses all possible M values, and the dissociation probability for a specific rotational state is averaged over all $(2J+1)$ projection states. However, when a strong electrostatic field is imposed above the solid surface, the relative weights of various M components change due to interaction between the molecular dipole and the field, and the molecular can thus be aligned. The effects of an external field on the DC dynamics have been observed experimentally,[40-41] but have not been elucidated theoretically.

An initial wave packet located in the reactant asymptote ($Z=Z_i$) can be defined as a product of a real Gaussian wave packet and internal state wavefunctions of the reactant:

$$\left|\Psi_i\right\rangle = Ne^{-(Z-Z_i)^2/2\delta^2}\cos k_i Z\left|\psi_{v_1v_2v_3,J_{K_aK_c}}\right\rangle \qquad (12)$$

where the internal state of the reactant is specified by the rotational and vibrational quantum numbers ($J_{K_aK_c}$ and (v_1,v_2,v_3)) and the initial momentum is given by $k_i=\sqrt{2ME_i}$, where E_i is the

initial mean kinetic energy. The wave packet is propagated using the Chebyshev propagator,[125-127]

$$\left|\Psi_k\right\rangle = 2D\hat{H}_s\left|\Psi_{k-1}\right\rangle - D^2\left|\Psi_{k-2}\right\rangle, \qquad k \geq 2\,, \tag{13}$$

where $\left|\Psi_1\right\rangle = D\hat{H}_s\left|\Psi_0\right\rangle$ and $\left|\Psi_0\right\rangle = \left|\Psi_i\right\rangle$. D is a damping function defined in the edges of the grid to impose outgoing boundary conditions. The Hamiltonian and energy are scaled as:

$$\hat{H}_s = (\hat{H} - \bar{H})/\Delta H\,, \quad E_s = (E - \bar{H})/\Delta H \tag{14}$$

to avoid the divergence of the Chebyshev propagator outside the range [-1, 1]. Here, the mean and half-width of the Hamiltonian, $\bar{H} = (H_{\max} + H_{\min})/2$ and $\Delta H = (H_{\max} - H_{\min})/2$, are estimated from its extrema $H_{\max}$ and $H_{\min}$. The initial state-specific dissociation probability is computed with the flux approach in the product channel at $r_2 = r_{2f}$:[128]

$$\begin{aligned} P^{J_{K_a K_c}}_{v_1 v_2 v_3}(E_c) = \frac{1}{2\pi\mu_2 \left|a_i(E_c)\right|^2 \Delta H^2 (1 - E_s^2)} \times \mathrm{Im}\Bigg[\Bigg\langle \sum_{k=0} (2 - \delta_{k0}) e^{-ik \arccos E_s} \Psi_k \Bigg| \\ \times \frac{\partial}{\partial r_2} \Bigg| \sum_{k'=0} (2 - \delta_{k'0}) e^{-ik' \arccos E_s} \Psi_{k'} \Bigg\rangle \Bigg]_{r_2 = r_{2f}}, \end{aligned} \tag{15}$$

where $a_i(E_c)$ is the energy amplitude of the initial wave packet at a given collision energy E_c.

For CH_4, the number of degrees of freedom increases to fifteen within the BOSS approximation. Even by neglecting the three coordinates as discussed above, there are still twelve coordinates. Unfortunately, it is still very difficult to carry out QD calculations for such a high-dimensional system, although recent work using the Multi-Configuration Time-Dependent Hartree (MCTDH) approach has shown some promise.[129] In our recent work, we have used an

eight-dimensional (8D) model to treat the DC of methane.[78] This model, originally proposed by Palma and Clary,[130] assumes that the CH_3 moiety remains in C_{3v} symmetry throughout the reaction. This is a reasonable approximation, which has been extensively used in gas phase X + CH_4 reactions.[131-135] For the DC of methane, the reduced-dimensional Hamiltonian is given as follows:[78]

$$\hat{H} = -\frac{1}{2M}\frac{\partial^2}{\partial Z^2} - \frac{1}{2\mu_r}\frac{\partial^2}{\partial r^2} + \frac{\hat{l}^2}{2\mu_r r^2} + \hat{K}_{CH_3}^{vib} + \hat{K}_{CH_3}^{rot} + V(Z, r, x, s, \theta_1, \varphi_1, \theta_2, \varphi_2)$$

(16)

As shown in Figure 2, Z is the distance between the CH_4 COM and the surface and r the distance between the atom H and CH_3 COM, with M and μ_r as the mass of CH_4 and H-CH_3 reduced mass. (θ_1, φ_1) are angles that define the rotation of CH_4 with respect to Z and (θ_2, φ_2) are angles that define the rotation of CH_3 with respect to r. $\hat{l} = \hat{J} - \hat{j}$ is the orbital angular momentum of atom H with respect to CH_3, with $\hat{J}$ and $\hat{j}$ as the rotational angular momenta of CH_4 and the non-reactive CH_3 moiety. The CH_3 vibration can be described in either the Cartesian coordinates (x, s) or scaled polar coordinates (q, γ), which can be interconverted.[132] $\hat{K}_{CH_3}^{vib}$ and $\hat{K}_{CH_3}^{rot}$ are the kinetic energy operators for the vibrational and rotational modes of the CH_3 moiety, and their forms can be found in the original publication.[78] Note that there is no coupling between the vibrational and rotational terms of the non-reactive CH_3 moiety. This 8D model allowed for the first time the inclusion of the two stretching vibrational modes (v_1 and v_3), albeit approximately. The description of the umbrella mode (v_4) is also included, but the deformation mode (v_2) is not because it is poorly defined in this model as the rocking motion tends to destroy the C_{3v} symmetry of the methyl moiety.

The wave packet can be expanded in terms of the basis sets for Z, r, q, γ and rotational basis functions. The former are represented in various forms of the DVR grids.[123] The rotations of the CH_3 and CH_4 moieties are described by Wigner functions in the coupled form. The definition of the initial wave packet, its propagation, and final projection are analogous to those in the H_2O case, and the detail of the model and numerics can be found in our original publication.[121] We have only investigated the rotationless methane, as experimental evidence suggested that the rotational excitation has small impact on the DC dynamics.[28,136]

The rigid-surface model ignores the motion of surface atoms and energy transfer between the impinging molecule and surface phonons, both representing severe approximations. Jackson and coworkers have investigated these effects extensively and carefully,[115-119] and we follow their approaches to remedy the deficiencies of the model. In particular, three corrections are made. First, the site dependence of the dissociation barrier is approximately taken into account by averaging higher-energy sites using an energy shifting scheme based on the harmonic oscillator.[137] This correction lowers the reaction probabilities because of the higher effective barrier. Second, the so-called "electronic coupling", which manifests by the "puckering" of surface atoms at the transition state, is modeled with a Boltzmann sampling of the positions of relevant surface atoms.[118-119] The premise of this approximation is based on the observation that the surface atom motion is not significantly affected by the reactive event, due to the large mass disparity between the metal atom and the molecule. As a result, the reaction can be simulated with the position of surface fixed at positions determined by the Boltzmann factor. This correction has a large impact on the reaction probabilities at low collision energies, due to the lower reaction barrier associated with the reconstruction on the surface.[115-117] It also introduces the dependence of reactivity on surface temperature. Finally, the "mechanical coupling", which

originates from the collisional energy transfer with the surface atom, is approximated by a surface-mass model.[110] In particular, this involves a shift of the Z coordinate in the PES and scaling of the molecular mass.[118-119]

IV. Sudden Vector Projection Model

The mode specificity in DC suggests that not all forms of energy are equal in promoting the reaction. This non-statistical feature of the DC dynamics can be traced to the different coupling strengths of the reactant modes with the reaction coordinate at the transition state. In the recently proposed Sudden Vector Projection (SVP) model,[57] the collision time is assumed to be much shorter than that required by intramolecular vibrational energy redistribution (IVR) in the impinging molecule. This is reasonable for molecules such as methane and water, as their densities of states are quite sparse, which lead to slow IVR.[138] Recently AIMD calculations of methane DC also verified that the reaction is close to the sudden regime.[52-56] In this sudden limit, the coupling of a reactant mode, whether is translational, rotational, or vibrational, with the reaction coordinate at the transition state can be approximated by the projection of the reactant normal mode vector ($\vec{Q}_i$) onto the reaction coordinate vector ($\vec{Q}_{RC}$): $P_i = \vec{Q}_i \cdot \vec{Q}_{RC} \in [0,1]$. The larger the projection, the stronger coupling, and thus the greater ability to enhance the reaction.

The SVP model emphasizes the importance of the reaction transition state in controlling mode specificity in chemical reactions,[58] in the same spirit as the venerable Polanyi's rules,[139] which were initially proposed for understanding mode specificity in atom-diatom reactions. Indeed, the descriptor of the barrier location in the latter is essentially equivalent to the SVP value (P_i), as we have shown for atom-diatom reactions.[57] On the other hand, the SVP model is more general, applicable to reactions with polyatomic reactants. Importantly, the SVP model

does not require the entire PES to make predictions and only information on the stationary points is needed.[140] This feature allows the survey of mode specificity of complex systems without mapping out the full-dimensional PESs.[141] Already, the SVP model has been applied to many activated reactions in the gas phase and at gas-solid interfaces, and its predictions have generally been borne out.[59]

The extension of the SVP model to DC on surfaces allows the prediction of additional dynamical features. For example, the choice of the displacements of COM coordinates as reactant vectors allows the examination of the effect of incident angles on the reactivity.[55,141] In addition, the projection of coordinates of surfaces atoms sheds light on their involvement in the reaction coordinate at the transition state.[141]

V. Dissociative Chemisorption

A. H_2O

The DC of H_2O, which forms chemisorbed H and OH species on the catalyst surface, is the initial step of steam reforming and WGS reaction.[3] It typically has a high barrier (0.5~1.0 eV relative to free H_2O far above the surface), representing the rate-limiting step in the low-temperature WGS reaction on Cu catalysts.[5] DFT studies of the water dissociation have been reported by many groups.[141-146] The main features of the reactive transition state are quite similar on different transition metal surfaces. As shown in Figure 3 for that on Ni(111), it is clear that the bond length of the dissociative O-H bond is significantly elongated, signaling a very late barrier. However, little is known until recently about the dynamics of this important heterogeneous process, either experimentally or theoretically.[147] The only experimental work on

dynamics was on the non-dissociative sticking of H_2O on Pt(110)-(1×2), where the kinetic energy (27 kJ/mol) is significantly below the dissociation barrier.[148]

In 2012, we proposed a high-dimensional model to describe the dynamics of water DC on the rigid Cu(111) surface.[77] In this model, six out of the nine coordinates are included, as shown in Figure 2. The only ones ignored are the lateral coordinates (*X* and *Y*) and the azimuthal angle (ϕ). This model, which is reasonable for close-packed surfaces such as the (111) facet, represents the first realistic treatment of H_2O DC. The inclusion of all vibrational degrees of freedom of the reactant molecule allowed us to examine its mode specificity. The six-dimensional (6D) PES was constructed from more than 25000 DFT points using a modified PIP method, in which the surface is approximated as a pseudo-atom with the *X*-*Y* coordinates fixed at the transition-state geometry. This PES represents a reasonably faithful representation of the DFT points, except for the product channel where the reduced-dimensional model becomes inadequate. In addition to the shallow physisorption well in the entrance channel, the PES is dominated by a late transition state, featuring an elongated O-H bond.

The quantum dynamics of both the ground and vibrationally excited states of H_2O were investigated using a six-dimensional Chebyshev wave packet method.[77] All three vibrational modes of H_2O are found to enhance the DC reactivity, and their vibrational efficacies are all larger than unity. In particular, the symmetric stretching mode has the largest vibrational efficacy, followed by the antisymmetric stretching and bending modes. The enhancement of the reactivity was rationalized by the vibrationally adiabatic mechanism,[122] but the mode specificity might be better understood with the SVP model (*vide infra*).[141] There is significant reactivity below the reaction barrier, suggesting that tunneling is the main reaction mechanism at low collision energies. We note in passing that similar mode specificity was observed by others using a much

cruder model.[149] The strong mode specificity in these theoretical studies strongly suggests that the DC process is dominated by dynamics and different forms of energy have different efficacies in promoting the reaction. Subsequently, this 6D model was used to study bond selectivity in the DC of HOD.[121] Our QD results clearly indicated that the excitation of the local mode vibration of either the OH or OD bond greatly promotes its cleavage, while inhibiting the cleavage of the other bond. The observed bond selectivity is also consistent with the SVP model.[141]

Further studies within this reduced-dimensional model explored the effect of rotational and orientational degrees of freedom of the H_2O reactant on the reactivity on an improved 6D PES.[122] After averaging the $(2J+1)$ degenerate M states in the absence of an external field, as displayed in the upper panel of Figure 4, it was shown that low-lying rotational excitations of H_2O all enhance the reaction to some extent. These notable rotational effects can presumably be traced to the strong anisotropy of the interaction PES. Indeed, water as an asymmetric top behaves very differently from the spherical CH_4 rotor, which has a very weak rotational effect (*vide infra*).[28] Interestingly, the initial orientation of the molecule also has a significant impact on reactivity, as shown in the lower panel of Figure 4. These results from our group[122] and others[149] indicated an remarkable orientational effect, namely the dependence of the reactivity on the projection of the rotational angular momentum on the surface normal (M).[122] This effect, which is not entirely surprising because of the well-defined transition state for the DC of water on transition metal surfaces, still awaits experimental verification.

The DC of water on transition metal surfaces bears much resemblance with reactions of H_2O with atomic species such as H and Cl. Both the H/Cl + $H_2O \rightarrow H_2$/HCl + OH reactions are dominated by late barriers and strong mode specificity and bond selectivity are well established.[150-161] As mentioned above, Polanyi's rules provided valuable guidance on the origin

of these non-statistical phenomena, but they have difficulties in making quantitative mode specific predictions, particularly for polyatomic molecules. However, the mode specificity and bond selectivity in these gas phase reactions can be rationalized by our recently proposed SVP model.[13] The SVP model[57,59] can also be used to explain the mode specificity and bond selectivity in DC of water. In Figure 5, projections of various reactant mode vectors onto the reaction coordinate vector at the appropriate transition state are shown for the DC of H_2O, D_2O, and HOD on Ni(111). It is clear from these figures that the stretching vibrational modes typically have the largest overlaps with the reaction coordinate. This is followed by the translational and bending modes. For HOD, the OH or OD vibration is well aligned with the corresponding transition states. Apart from the bending mode, these SVP predictions are consistent with the QD results discussed above, and are very similar to those for the H/Cl + H_2O/D_2O/HOD reactions in the gas phase.[58] The underestimation of the bending mode efficacy in this and other systems might be related to the fast IVR in the angular degrees of freedom.[59]

Our theoretical studies have since stimulated detailed an experimental exploration of mode specificity in DC of water. Using a molecular beam apparatus, Hundt *et al*. measured the initial sticking probabilities of D_2O on Ni(111) at several kinetic energies in the direction of the surface normal.[48] This experimental study revealed that the DC reaction is direct and excitations of the antisymmetric stretching mode of D_2O to its fundamental and first overtone levels significantly enhance the reactivity at all energies. To better understand the experimental findings, we have developed a 6D PES for water interacting with rigid Ni(111), using essentially the same protocol as in the Cu(111) case.[48] While some quantitative differences exist, the PES for the H_2O/Ni(111) system is qualitatively similar to that for its H_2O/Cu(111) counterpart, again

featuring a late barrier. This PES is displayed in Figure 3 as a function of Z and r_2 with other coordinates relaxed, with the transition-state geometry given in the inset.

Wave packet dynamics within the 6D model was performed for both the ground and vibrationally excited states of D_2O.[48] Furthermore, the QD reaction probabilities were corrected for several approximations in our model. First, the dependence of the barrier height on the impact site was taken into account approximately using an energy shifting scheme based on the harmonic oscillator model.[137] This correction lowers the reactivity because of the higher effective barrier. As discussed below, this simple model is not entirely valid, as shown by later full-dimensional studies.[55,96] Second, the "electronic" coupling effect, originating from the movement of surface Ni atoms, was included in a simple fashion, following Jackson.[50] This correction has a large effect on the reactivity, as it increases the reactivity at low collision energies and lowers that at higher collision energies. Finally, the "mechanical" coupling effect stemming from energy transfer from the impact of the molecule on metal atoms, was taken into consideration using a surface-mass model.[50] The effect of this final correction is relatively small.

Importantly, the experimentally measured initial sticking probabilities placed a strong constraint on the theoretical model. It was found that the PES constructed with DFT points with the PW91 functional has too low a barrier, leading to overestimation of the measured reactivity. Such underestimations of reaction barrier by the PW91 functional have been noted in other DC systems.[25,162] To correct the underestimation of the barrier height, we have modified the PES using a simple Z-dependent scaling scheme. The final theoretical results are compared with the measured initial sticking probabilities in Figure 6. The agreement is semi-quantitative.

It should be noted that the laser-off results in Figure 6 represent a Boltzmann average of contributions from many low-lying D_2O vibrational states. This is because the nozzle temperature in the experiment was 573, 673, and 773 K for the three kinetic energies of the impinging molecule.[48] While the excited vibrational states of D_2O have relatively small populations at these temperatures, their reactivities are very large comparing with that of the ground vibrational state. As a result, the initial sticking probability for the laser-off experiment is dominated by the excited vibrational levels of the D_2O molecule. The situation here is quite similar to the $H + H_2O$ reaction in which the low temperature rate coefficients are dominated by excited vibrational levels of the H_2O reactant.[157] This realization is important for steam reforming, as the major reactive events at the operating temperature (700-1100^{o}C) are likely due to vibrationally excited water.

Very recently, we have developed a full-dimensional model for the DC of water on rigid Ni(111), in which the 9D PES was fit to over 25000 DFT points using the PIP-NN method.[96] The relatively small number of points needed and the small (20 meV) RMSE reflect the power of symmetry adaptation. This full-dimensional PES allowed us to examine not only mode specificity, but also the dependence of the reactivity on the impact site and incident angles.[96] Since a 9D QD calculation is still not feasible, we have employed a QCT method to explore these issues, but restricting to relatively high translational energies. In addition, no correction of the lattice effects was performed in this preliminary study. It is clear from Figure 7 that the previously observed high vibrational efficacies for all vibrational modes of D_2O on the 6D PES were reproduced on this 9D PES, which validates the adequacy of the reduced 6D model for studying the DC of water.

Surprisingly, it was found for DC of water that the site-specific reactivity is not a simple function of the barrier height. Rather, it depends on the PES topography in a complex fashion, as seen in Figure 8. It turns out that the top site, despite its low barrier height, is least reactive. This is because the corresponding transition state is very tight and the PES at small Z values shows a weak coupling for energy flow from the translational coordinate to the reaction coordinate, as illustrated in Figure 8. Despite their higher barriers, on the other hand, the hcp and bridge sites are much more reactive, because the corresponding transition states are much looser and the coupling between the Z and r_2 coordinates are much stronger at small Z values. This is also shown in Figure 8. A similar conclusion has also been reached by Zhang and coworkers for the DC of HCl on Au(111) surface.[87] On the other hand, the site specificity is quite different from the behavior in methane DC, in which the dissociation is largely determined by the barrier height.[54-55] These observations indicate that the harmonic correction scheme for site average[137] might not be reliable if a quantitative understanding is desired.[55]

Furthermore, we have examined the effects of incident angles in the DC dynamics of H_2O. An earlier SVP survey of water DC processes on various transition metal surfaces has predicted varying levels of dependence on the incident angles.[141] These predictions have been borne out by the QCT calculations on the 9D PES for Ni(111).[96] In Figure 9, two sets of calculations have been performed for H_2O impinging on the surface. One varied the angle from the surface normal (θ) with a fixed kinetic energy, while the other varied the kinetic energy at different θ values but fixing the kinetic energy projection on the surface normal. It was found in former case that the dissociation probability decreases with increasing the incident angle, while in later case that the dissociation probability increases with the incident angle. These results show that normal scaling is not kept for this process and the momenta along the surface plane

have a promotional effect on the reactivity, because they couple with the reaction coordinate at the transition state. This theoretical prediction is yet to be verified by experiment.

B. CH_4

The DC of methane to form chemisorbed H and CH_3 represents the initial and rate-limiting step in the steam reforming of natural gas,[6] which is the major industrial process for hydrogen production. The dynamics of methane DC on various transition metal surfaces, such as Ni and Pt, has been extensively studied by several experimental groups. Earlier work indicated that the DC process on most transition metal surfaces is direct and activated by kinetic energy, in many cases with normal scaling.[163-168] Later studies also found evidence of vibrational enhancement.[164-169] However, the mode specificity and bond selectivity did not emerge clearly until the molecular beam studies with the impinging molecule prepared in single quantum states.[26-45] The nine vibrational degrees of freedom in methane offer a unique opportunity to investigate their efficacies in promoting the DC reaction. Indeed, strong mode specificity and bond selectivity have been identified and as a result, the methane DC has become an important proving ground for studying dynamics of molecular surface reactive scattering processes.[9,18,25,49-50]

Like in the DC of water, the DC of methane features a significant energy barrier (0.5 - 1.0 eV) with an elongated C-H bond, as found in DFT calculations on various transition metal surfaces.[115-117,170-175] The transition-state geometry on Ni(111) is shown in Figure 3. This late barrier is suggestive of enhancement of reactivity by the stretching vibrations that involve the breaking C-H bond. Indeed, experimental evidence has shown high efficacies for stretching modes in CH_4 and its deuterated isotopomers. In addition, these DFT studies have revealed that

the metal atom beneath the molecule puckers up at the transition state, suggesting the involvement of the surface lattice motion.

Jackson and coworkers have carefully investigated the lattice effects in the DC of methane.[50] This extensive body of work identified two major forms of coupling.[115-119,137] The "electronic" coupling due to the puckering of the substrate metal atom immediately below the impinging methane near the transition state signaling the participation of surface phonons in the reaction. On the other hand, the "mechanical" coupling stems from the finite mass of the surface atom and its collisional energy transfer from the incoming methane. The former can be effectively treated within a sudden model[118-119] with different Z positions of the surface atom. The final result is obtained by weighting the Z distribution by the Boltzmann factor. This sudden model is appropriate because the surface atom is too heavy to follow the fast molecular motion. On the other hand, the fluctuation of its position is affected by the surface temperature. As the motion of the surface atom effectively lowers the reaction barrier, this model explains at a microscopic level the experimentally observed surface temperature effects.[37,164,167] The mechanical coupling is relatively easy to model, which essentially involves shifting the PES in the Z direction and a scaling of the molecular mass.[118-119]

With few exceptions,[111,176] earlier theoretical models for methane DC were based on the pseudo-diatom approximation, in which the methyl moiety is treated as a pseudo atom.[109-110,112,115] If the pseudo-diatom is not allowed to rotate, two degrees of freedom are sufficient within the BOSS approximation.[110] The inclusion of the rotational degree of freedom increases the dimensionality to three.[112] More sophisticated treatment of the rotational coordinates have been proposed.[114,177] More recently, reduced-dimensional models with 2, 3, and 4 coordinates have been investigated.[120] Apparently, such reduced-dimensional models are incapable of

addressing important issues such as the differences between symmetric and antisymmetric stretching modes. In addition, these earlier studies have mostly been based on empirical or semi-empirical PESs.

Jackson and coworkers have recently introduced a full-dimensional, albeit approximate, model for methane DC,[137,178-179] based on the reaction path Hamiltonian (RPH) of Miller, Handy, and Adams.[180] In this RPH approach, the PES is approximated along the reaction coordinate by harmonic potentials of (3*N*-1) generalized normal modes, where *N* is the number of atoms in the system. The rotational modes of the molecule can be approximately treated within the adiabatic approximation, but the vibrational non-adiabatic couplings are required in order to give correct results. Although this model represents an approximate description of the reactive system near the minimum energy path, it offers a full-dimensional perspective of the potential landscape. Such RPH PESs have been developed before,[113,181] but the novel aspect of Jackson's approach is to model the reaction dynamics within a QD framework by expanding the wave packet in terms of the adiabatic normal mode basis. Starting with an initial vibrational state of methane above the metal surface, the propagation of the close-coupled wave packet with the RPH framework allows not only the reaction in the adiabatic channel, but also non-adiabatic ones *via* transitions to other vibrational channels. In fact, the non-adiabatic pathways typically dominate the reaction, as discussed below. Finally, the single site reaction probabilities are corrected for site and lattice effects, as described above.[50] Using this model, Jackson and coworkers have qualitatively reproduced the experimental observations on mode specificity and bond selectivity on various transition metal surfaces.[182-184] In the upper panel of Figure 10, for example, the initial sticking probabilities of vibrationally ground and first excited states of methane on Ni(100) are shown as a function of the incident translational energy, where mode specificity is apparent. The

reasonable agreement with the measured initial sticking probabilities suggests that the RPH approach captures the salient features of the DC process.

Although the RPH approach is full-dimensional, it is only accurate near the minimum energy path. A quantitative description of the molecule-surface interaction can only be achieved with a fully coupled global PES. Indeed, the lack of such PESs represented a major bottleneck in understanding the DC dynamics of methane. Efforts in this direction have been made recently.[120,185] For example, we have developed a twelve-dimensional (12D) PES for methane interacting on rigid Ni(111).[78] Like in our 6D model for water on transition metal surfaces,[77] the only coordinates neglected in the 12D model are the lateral (X and Y) coordinates and the azimuthal angle (ϕ). The neglect of the lateral coordinates is consistent with the observed "normal energy scaling" in methane dissociative chemisorption on transition metal surfaces.[9] In this 12D model, all vibrational coordinates of methane are included. The global PES was constructed using a modified PIP method from more than 36000 DFT points in twelve dimensions. It provides a reasonably faithful description of most of the reaction channels, except for the product region where the reduced-dimensional model is not expected to be accurate.

The 12D PES has since facilitated both QD and QCT studies of the methane DC dynamics. The QD calculations were done with the 8D model discussed in Sec. III, which includes an approximate description of all four normal modes of methane.[78] After correcting the impact site and lattice effects according to the protocol of Jackson and coworkers,[50] the calculated initial sticking probabilities are in semi-quantitative agreement with the experimental measurements,[78] as shown in Figure 11. The calculated vibrational efficacies for all methane vibrational modes are listed in Table I, which are in reasonably good agreement with the available experimental values. It is interesting to note that the symmetric stretching mode has the

highest vibrational efficacy, followed closely by the antisymmetric stretching mode. Both are more effective than the translational mode in promoting the reaction. The bending modes have relatively small vibrational efficacies. The good theory-agreement suggests that this reduced dimensional model captures the essential physics of the methane DC dynamics.

Subsequently, the mode specificity and bond selectivity of various partially deuterated methane isotopomers were investigated using a QCT method on the same 12D PES.[186] The 12D model allowed the investigation the DC dynamics of not only CH_4, but also CHD_3 and CH_2D_2 which cannot be treated with the 8D model discussed above. The aim is to understand the trends in the DC dynamics, so only the DC at high kinetic energies was examined, and neither site nor lattice correction was incorporated. It was shown that the mode specificity in the DC of CH_4 is quite similar to that observed in the 8D QD calculations on the same PES, although the QCT results underestimate the reactivity somewhat. In the case of CHD_3, the excitation of the C-H stretching mode (v_1) significantly enhances the cleavage of the C-H bond, while excitations of the CD_3 symmetric (v_2) and antisymmetric stretching (v_4) modes promote the dissociation of a C-D bond. This is in agreement with the experimental work of Utz and coworkers.[36] The situation for CH_2D_2 is more complex, because this molecule is better described in the local mode regime. Our QCT results indicated that the excitation of one C-H bond with two quanta leads to a larger C-H dissociation probability at low energies than exciting both C-H bonds with one quanta. In addition, both vibrational excited states show substantial enhancement of the reaction over the ground vibrational state of the molecule. This is consistent with the experimental results of Beck and coworkers.[31]

To understand the mode specificity and bond selectivity in methane DC, we again rely on the SVP model. In Figure 5, the alignment of reactant normal mode vectors of CH_4, CHD_3 and

CH_2D_2 on Ni(111) with the reaction coordinate at the transition state is displayed. Our model predicts the vibrational efficacy for CH_4 in the order: $v_1>v_3>v_2>v_4$, in agreement with both theoretical and experimental observations. For CHD_3 and CH_2D_2, the four transition states are nonequivalent, but the corresponding SVP values do predict the observed and calculated mode specificity and bond selectivity. We also note here the these DC processes share many similarities with the reactions between methane and atomic reactants such as H and Cl in the gas phase,[187] where mode specific and bond selective chemistry is well established.[188-196]

Finally, we note in passing that Harrison and coworkers have advanced a statistical approach to methane DC processes.[197-199] While reproducing many observed properties, the statistical models are fundamentally incompatible with the mode specific dynamics supported by the overwhelming experimental and theoretical evidence. These state-resolved studies clearly indicate that the energy flow in the reactants is slow relative to the collisional time scale, and thus quite far from the ergodic limit assumed by statistical models.[138] This is true despite the fast energy flow within the metal itself, either in the form of phonons or electron-hole pairs, because the coupling to the surface "bath" modes only takes place when the molecule is sufficiently close the surface and thus the transition state. The key to the existence of mode specificity can thus be attributed to two major factors.[59] First, the sparse density of states of the impinging molecule, such as water or methane, which lead to a slow IVR; and second, the rapid collision time between the molecule and the surface, which precludes energy flow between the molecule and surface. Nevertheless, such statistical treatments might be appropriate for DC of molecules with a precursor mechanism, in which the randomization is expected to be rather complete.

C. Sudden and Adiabatic Limits

The SVP model can be considered as a generalization of the venerable Polanyi's rules.[59] As we demonstrated in gas phase atom-diatom reactions, the coupling of the reactant modes with the reaction coordinate at the transition state used in the SVP model as the descriptor for estimating their abilities to promote the reaction is indeed correlated with the descriptor used by Polanyi, namely location of the barrier.[57] However, the location of barrier may not be unique nor necessarily accurate, as demonstrated by several recently found exceptions.[200-201] More importantly, the SVP model is amenable to polyatomic molecules. The success of the SVP model in predicting mode specificity and bond selectivity in DC processes clearly indicated the prowess of this simple, but insightful model.

The mode specificity in DC reactions has also been rationalized using the RPH model, which is based on a vibrationally adiabatic representation.[78,113] Taking the example of methane, the symmetric stretching mode localizes to a C-H vibration towards the surface as the molecule approaches the surface. Near the transition state, the frequency of this mode drops substantially, reflecting "mode softening". As a result, the corresponding barrier for the adiabatic potential is lowered relative to that of the ground vibrational state of the reactant. This barrier-lowering effect, which is also seen for the umbrella mode of methane, was taken as the cause of the enhancement of reactivity. On the other hand, the three degenerate antisymmetric stretching modes of the methane reactant are localized into three C-H vibrations pointing away from the surface as the molecule approaches the surface, and they do not experience "mode softening". Their promotional effects can only be rationalized by invoking vibrationally non-adiabatic transitions to other vibrational states that have lower barriers.

This analysis based on the RPH Hamiltonian intrinsically assumes the collisional process is very slow, close to the adiabatic limit. Under such circumstances, the reactant molecule can

thus adjust its vibrational modes along the reaction coordinate. This is clearly not the case in the DC processes discussed above. The high kinetic energy makes the adiabatic limit unattainable,[138] and as a result, the DC processes is much closer to the sudden limit. Indeed, there is ample evidence from both QCT[186] and AIMD studies[52-56] of activated DC processes that strongly suggests the vibration of the impinging molecule is minimally perturbed before reaching the transition state, thus favoring the sudden limit. Wave packet studies based on RPH PESs have also indicated that the dynamics is intrinsically not adiabatic and most reactivities derive from transitions amongst the adiabatic vibrational channels.[49,137,182-184] This is clearly shown in the lower panel of Figure 9, in which the non-adiabatic reaction probabilities obtained from the RPH model for methane DC on Ni(100) are far higher than the adiabatic ones, even for the symmetric stretching mode v_1, whose enhancement is usually explained in terms of adiabatic mode-softening. We emphasis in passing that the RPH wave packet approach is capable of handling vibrationally non-adiabatic dynamics because it explicitly incorporates the non-adiabatic couplings among the vibrational modes during propagation.

These two models are also related as both emphasize the reaction coordinate at the transition state. The key difference lies in the behavior of the modes of the reactant as it approaches the surface. In the adiabatic limit, these modes change slowly and adiabatically as the system moves from the reactant asymptote to the transition state so that the vibrational non-adiabatic coupling due to the curvature of the reaction coordinate can be ignored. In the sudden limit, however, the fast approaching reactant leaves no time for it to adjust its internal energy, and as a result, only the direct projections of the reactant mode vectors onto the reaction coordinate at the transition state matter. In principle, both the sudden and adiabatic limits may

exist, but the DC processes discussed here are clearly closer to the sudden limit, due mainly to the slow IVR of the reactants.

VI. Conclusions

In this review, we have summarized the recent advances in dynamical studies of DC processes involving polyatomic molecules on transition metal surfaces. Our focus has been placed on two prototypical molecules of both academic and industrial importance, namely water and methane, as well as their deuterated isotopomers. In the former, first-principles studies have found significant mode specificity and bond selectivity, which have since stimulated new experimental exploration. In turn, the measurements of the initial sticking probabilities have provided a stringent test of the theoretical model and helped to improve it. In the latter case, theoretical models have been greatly improved to include all vibrational degrees of freedom, and they provided valuable insights concerning the mode specificity and bond selectivity in the DC dynamics observed by numerous experimental measurements. These advances clear demonstrated that the non-statistic molecule-surface dynamics is quite prevalent.

The progress in theoretical understanding of the DC dynamics has been made possible by two notable advances. The first is the construction of high-dimensional PESs that describe globally the interaction between molecules and metal surfaces. These global PESs are faithful analytic representations of first-principles electronic energies in a vast configurational space, thus not relying on empirical considerations and/or approximations. The mathematic problem of high-fidelity representation of a discrete set of points is not straightforward for high-dimensional systems and the difficulties are compounded by issues related to symmetry adaptation. However, once built, they not only allow efficient QCT exploration of dynamical issues that are still

difficult to sample with AIMD, but more importantly also facilitate non-local QD characterization of the dynamics. Our solution to this PES fitting problem is the PIP-NN method, which accounts for the periodicity of the surface as well as the permutation symmetry of the molecule. The PIP-NN approach is rigorous, simple, accurate, efficient, easy to implement, and quite general. We expect wide applications in surface dynamics.

The second advance is high-dimensional QD approaches based on wave packet propagation. The QD approach has been applied with 6 and 8 dimensions and revealed important dynamical features in the DC processes. Despite these successes, however, a full-dimensional treatment remains elusive, if not impossible, because of the exponential scaling of the QD approach. Further progress might be possible using approximate QD methods such as MCTDH. It may also be possible to take advantage of known properties of the DC dynamics. For example, the total reactivity in certain problems can be approximated by a site-average model.[202] This is a reasonable approximation because there is ample evidence indicating that the collision process is largely sudden in the lateral (*X* and *Y*) coordinates. Such models have been shown to work well in diatomic DC dynamics.[87,203] The application of the site-average model to water DC would reduce the QD calculations to multiple 7D ones, which are entirely manageable.

The accumulation of both experimental and theoretical knowledge on the DC dynamics has greatly advanced our understanding of these important reactions. The mode specificity and bond selectivity observed in these processes can be readily understood in terms of the SVP model,[59] which can be considered as a generalization of Polanyi's rules. Attributing the ability of a reactant mode in promoting the reaction to the projection of its normal mode vector onto the reaction coordinate vector at the transition state, the SVP model has been quite successful in predicting the mode specificity and bond selectivity in many reactive processes. The general

success of the SVP model is a strong indicator that this model captures the essential physics in these direct and activated reactions. It also argues for the sudden nature of these processes on the basis of slow IVR in the molecules under investigation, supported by recent AIMD calculations.

Despite the rapid progress summarized in the review, it is clear that there are still many issues that are not yet well understood. One is the rotational and orientational effects, which have seldom been explored theoretically. However, there have been several experimental studies on these topics. For example, Beck and coworkers have demonstrated a strong steric effect in the DC of methane, using an IR laser that polarizes either parallel or perpendicular to the surface.[40-41] This steric effect, which provides important information on the DC dynamics, has so far defied a theoretical explanation. This is partly because the involvement of rotational and orientational degrees of freedom significantly complicates the dynamical model. More theoretical attention should be paid to these important issues.

So far, almost all DC studies have been restricted to close-packed surfaces. On the other hand, it is known that surface defects often play an important, sometimes dominant role, in catalysis.[1] Very little is known about the effects of steps, kinks, and vacancies on DC dynamics, although some progress has recently been made.[23,38-39] A significant dependence on incident angles has been observed in the mode-specific DC of methane on the highly corrugated Pt(110)-(1×2) surface.[39] In addition, many catalysis processes are now performed on alloy surfaces, and our knowledge on the dynamics of DC processes on these surfaces is also quite limited.[204] Future studies in both experiment and theory would undoubtedly improve our understanding of these scenarios more relevant to catalysis. In addition, the DC systems studied so far are almost exclusively direct. Recent studies have indicated that a significant pre-reaction well on Ir(111) might induce trapping for methane.[205-206] The treatment of DC mediated by tapping will be a

challenge for dynamical calculations, as the lifetime of the trapped species can be quite long, and energy transfer with the substrate is unavoidable.

Another important issue is the role of energy transfer during the collisional process, and more generally the role of surface phonon in molecule-surface interactions. So far, this is approximately treated using various models, but a proper treatment is required if a complete understanding of the DC dynamics is to be achieved. AIMD certainly provides a first-principles approach, but is very computationally expensive. The reaction force field method might offer a more efficient alternative.[185] Mixed quantum-classical models also represent a promising venue of research.[119] A related issue is the potential participation of electron-hole pairs, which has been found prevalent in NO scattering.[17,19] Although the latter phenomenon has been dismissed in most DC systems, its complete exclusion is probably not warranted. More studies on when these effects become important will be very valuable.

To summarize, much progress has been made in our theoretical, in particular quantum mechanical, understanding of molecular dissociation dynamics on transition metal surfaces. These new insights will undoubtedly help us to better understand a wide range of processes involving gas phase molecules and metal surfaces, including catalysis. However, to achieve these goals, new theoretical models and methods will need to be developed.

Acknowledgements: The work at UNM was supported by the US National Science Foundation (Grant Nos. CHE-0910828 and CHE-1462109 to HG). MY acknowledges the support of National Natural Science Foundation of China (21221064 and 21373266). DX is supported by the National Natural Science Foundation of China (21133006, 21273104, and 91421315) and the

Ministry of Science and Technology (2013CB834601). BJ and HG would like to thank Rainer Beck, Bret Jackson, Geert-Jan Kroes, Ashwani Tiwari, and Art Utz for many stimulating discussions.

Bios

Bin Jiang did his undergraduate and graduate studies at Nanjing University, China. After receiving his Ph.D. in Physical Chemistry in 2012 with Prof. Daiqian Xie, he has been working as a postdoctoral fellow with Professor Hua Guo at Department of Chemistry and Chemical Biology, University of New Mexico, USA. In 2015, he joined the faculty of University of Science and Technology of China. He is currently interested in high-dimensional *ab initio* potential energy surfaces, non-adiabatic dynamics, and chemical dynamics in the gas phase and/or at gas-surface interfaces.

Minghui Yang received his Ph.D in Chemistry from Sichuan University, China in 1997, under Profs. Guosen Yan and Daiqian Xie. He was then a postdoctoral with Prof. Yuansheng Jiang in Nanjing University (1997-1999) and with Prof. Donghui Zhang in National University of Singapore (2000-2004). In 2004 he joined Wuhan Institute of Physics and Mathematics, Chinese Academy of Sciences. His current research focuses on quantum dynamics of polyatomic reactions and molecular spectra.

Daiqian Xie received his B.S. from Sichuan University in 1983 and Ph. D. in Physical Chemistry from Jilin University in 1988. After a postdoctoral appointment at Jilin University from 1988 to 1991, he joined the faculty of Sichuan University for 10 years. He is Professor of Chemistry at Nanjing University since 2011. His research focuses on the quantum state resolved dynamics of photodissociation, small molecule collisions, molecular spectroscopy, and dissociative chemisorption on metal surfaces. He has (co-)authored about 300 papers in international journals.

Hua Guo received his D. Phil. In Theoretical Chemistry from Sussex University, UK, under Prof. John Murrell in 1988. After a postdoctoral stint with Prof. George Schatz at Northwestern University, he started his independent career at University of Toledo in 1990. He currently holds the positions of Professor of Chemistry and Physics at University of New Mexico. His current research interests are primarily on molecular spectroscopy, chemical kinetics, and quantum and classical dynamics of gas-surface and gas phase reactions. He is an elected fellow of the American Physical Society and the author of more than 350 publications.

References:

(1) Somorjai, G. A. *Introduction to Surface Chemistry and Catalysis*; Wiley: New York, 1994.
(2) Nilsson, A.; Petersson, L. G. M.; Nørskov, J. K. *Chemical Bonding at Surface and Interfaces*; Elsevier: Amsterdam, 2008.
(3) Chorkendorff, I.; Niemantsverdriet, J. W. *Concepts of Modern Catalysis and Kinetics*; Wiley-VCH: Weinheim, 2003.
(4) Ertl, G. *J. Vac. Sci. Technol. A* **1983**, *1*, 1247.
(5) Ovesen, C. V.; Stoltze, P.; Nørskov, J. K.; Campbell, C. T. *J. Catal.* **1992**, *134*, 445.
(6) Rostrup-Nielsen, J. R. In *Catalysis, Science and Technology*; Anderson, J. R., Boudart, M., Eds.; Springer-Verlag: Berlin, 1984; Vol. 5.
(7) Gross, A. *Surf. Sci. Rep.* **1998**, *32*, 291.
(8) Crim, F. F. *Acc. Chem. Res.* **1999**, *32*, 877.
(9) Juurlink, L. B. F.; Killelea, D. R.; Utz, A. L. *Prog. Surf. Sci.* **2009**, *84*, 69.
(10) Crim, F. F. *Faraday Discuss.* **2012**, *157*, 9.
(11) Czakó, G.; Bowman, J. M. *J. Phys. Chem. A* **2014**, *118*, 2839.
(12) Liu, K. *J. Chem. Phys.* **2015**, *142*, 080901.
(13) Li, J.; Jiang, B.; Song, H.; Ma, J.; Zhao, B.; Dawes, R.; Guo, H. *J. Phys. Chem. A* **2015**, *119*, 4667.
(14) Rettner, C. T.; Auerbach, D. J.; Tully, J. C.; Kleyn, A. W. *J. Phys. Chem.* **1996**, *100*, 13021.
(15) Sitz, G. O. *Rep. Prog. Phys.* **2002**, *65*, 1165.
(16) Kleyn, A. W. *Chem. Soc. Rev.* **2003**, *32*, 87.
(17) Wodtke, A. M.; Matsiev, D.; Auerbach, D. J. *Prog. Surf. Sci.* **2008**, *83*, 167.
(18) Beck, R. D.; Utz, A. L. In *Dynamics of Gas-Surface Interactions*; Muino, R. D., Busnengo, H. F., Eds.; Springer: Heidelberg, 2013.
(19) Golibrzuch, K.; Bartels, N.; Auerbach, D. J.; Wodtke, A. M. *Annu. Rev. Phys. Chem.* **2015**, *66*, 399.
(20) Christmann, K. *Surf. Sci. Rep.* **1988**, *9*, 1.
(21) Kroes, G.-J. *Prog. Surf. Sci.* **1999**, *60*, 1.
(22) Kroes, G.-J.; Gross, A.; Baerends, E.-J.; Scheffler, M.; McCormack, D. A. *Acc. Chem. Res.* **2002**, *35*, 193.
(23) Olsen, R. A.; Juurlink, L. B. F. In *Dynamics of Gas-Surface Interactions*; Muino, R. D., Busnengo, H. F., Eds.; Springer: Heidelberg, 2013.
(24) Kroes, G.-J. *Science* **2008**, *321*, 794.
(25) Kroes, G.-J. *Phys. Chem. Chem. Phys.* **2012**, *14*, 14966.
(26) Juurlink, L. B. F.; MaCabe, P. R.; Smith, R. R.; DeCologero, C. L.; Utz, A. L. *Phys. Rev. Lett.* **1999**, *83*, 868.
(27) Juurlink, L. B. F.; Smith, R. R.; Utz, A. L. *J. Phys. Chem. B* **2000**, *104*, 3327.
(28) Juurlink, L. B. F.; Smith, R. R.; Utz, A. L. *Faraday Disc.* **2000**, *117*, 147.
(29) Higgins, J.; Conjusteau, A.; Scoles, G.; Bernasek, S. L. *J. Chem. Phys.* **2001**, *114*, 5277.
(30) Schmid, M. P.; Maroni, P.; Beck, R. D.; Rizzo, T. R. *J. Chem. Phys.* **2002**, *117*, 8603.
(31) Beck, R. D.; Maroni, P.; Papageorgopoulos, D. C.; Dang, T. T.; Schmid, M. P.; Rizzo, T. R. *Science* **2003**, *302*, 98.
(32) Smith, R. R.; Killelea, D. R.; DelSesto, D. F.; Utz, A. L. *Science* **2004**, *304*, 992.

(33) Juurlink, L. B. F.; Smith, R. R.; Killelea, D. R.; Utz, A. L. *Phys. Rev. Lett.* **2005**, *94*, 208303.
(34) Maroni, P.; Papageorgopoulos, D. C.; Sacchi, M.; Dang, T. T.; Beck, R. D.; Rizzo, T. R. *Phys. Rev. Lett.* **2005**, *94*, 246104.
(35) Bisson, R.; Sacchi, M.; Dang, T. T.; Yoder, B.; Maroni, P.; Beck, R. D. *J. Phys. Chem. A* **2007**, *111*, 12679.
(36) Killelea, D. R.; Campbell, V. L.; Shuman, N. S.; Utz, A. L. *Science* **2008**, *319*, 790.
(37) Killelea, D. R.; Campbell, V. L.; Shuman, N. S.; Utz, A. L. *J. Phys. Chem. C* **2009**, *113*, 20618.
(38) Bisson, R.; Sacchi, M.; Beck, R. D. *Phys. Rev. B* **2010**, *82*, 121404(R).
(39) Bisson, R.; Sacchi, M.; Beck, R. D. *J. Chem. Phys* **2010**, *132*, 094702.
(40) Yoder, B. L.; Bisson, R.; Beck, R. D. *Science* **2010**, *329*, 553.
(41) Yoder, B. L.; Bisson, R.; Hundt, P. M.; Beck, R. D. *J. Chem. Phys* **2011**, *135*, 224703.
(42) Chen, L.; Ueta, H.; Bisson, R.; Beck, R. D. *Faraday Disc.* **2012**, *157*, 285.
(43) Chen, N.; Huang, Y.; Utz, A. L. *J. Phys. Chem. A* **2013**, *117*, 6250.
(44) Ueta, H.; Chen, L.; Beck, R. D.; Colon-Diaz, I.; Jackson, B. *Phys. Chem. Chem. Phys.* **2013**, *15*, 20526.
(45) Hundt, P. M.; van Reijzen, M. E.; Ueta, H.; Beck, R. D. *J. Phys. Chem. Lett.* **2014**, *5*, 1963.
(46) Luntz, A. C. *J. Chem. Phys.* **2000**, *113*, 6901.
(47) Crim, F. F. *J. Phys. Chem.* **1996**, *100*, 12725.
(48) Hundt, P. M.; Jiang, B.; van Reijzen, M.; Guo, H.; Beck, R. D. *Science* **2014**, *344*, 504.
(49) Jackson, B. In *Dynamics of Gas-Surface Interactions*; Muino, R. D., Busnengo, H. F., Eds.; Springer: Heidelberg, 2013.
(50) Nave, S.; Tiwari, A. K.; Jackson, B. *J. Phys. Chem. A* **2014**, *118*, 9615.
(51) Greeley, J.; Nørskov, J. K.; Mavrikakis, M. *Annu. Rev. Phys. Chem.* **2002**, *53*, 319.
(52) Sacchi, M.; Wales, D. J.; Jenkins, S. J. *J. Phys. Chem. C* **2011**, *115*, 21832.
(53) Sacchi, M.; Wales, D. J.; Jenkins, S. J. *Phys. Chem. Chem. Phys.* **2012**, *14*, 15879.
(54) Nattino, F.; Ueta, H.; Chadwick, H.; van Reijzen, M. E.; Beck, R. D.; Jackson, B.; van Hemert, M. C.; Kroes, G.-J. *J. Phys. Chem. Lett.* **2014**, *5*, 1294.
(55) Jackson, B.; Nattino, F.; Kroes, G.-J. *J. Chem. Phys.* **2014**, *141*, 054102
(56) Sacchi, M.; Wales, D. J.; Jenkins, S. J. *Comput. Theo. Chem.* **2012**, *990*, 144.
(57) Jiang, B.; Guo, H. *J. Chem. Phys.* **2013**, *138*, 234104.
(58) Jiang, B.; Guo, H. *J. Am. Chem. Soc.* **2013**, *135*, 15251.
(59) Guo, H.; Jiang, B. *Acc. Chem. Res.* **2014**, *47*, 3679.
(60) Zhu, X.-Y. *Annu. Rev. Phys. Chem.* **1994**, *45*, 113.
(61) Guo, H.; Saalfrank, P.; Seideman, T. *Prog. Surf. Sci.* **1999**, *62*, 239.
(62) Nieto, P.; Pijper, E.; Barredo, D.; Laurent, G.; Olsen, R.; Baerends, E. J.; Kroes, G.-J.; Farias, D. *Science* **2006**, *312*, 86.
(63) Juaristi, J. I.; Alducin, M.; Muiño, R. D.; Busnengo, H. F.; Salin, A. *Phys. Rev. Lett.* **2008**, *100*, 116102.
(64) Baule, B. *Ann. Phys.* **1914**, *349*, 145.
(65) Gamallo, P.; Martin-Gondre, L.; Sayós, R.; Crespos, C.; Larrégaray, P. In *Dynamics of Gas-Surface Interactions*; Muino, R. D., Busnengo, H. F., Eds.; Springer: Heidelberg, 2013.
(66) McCreery, J. H.; Wolken, G. *J. Chem. Phys.* **1975**, *63*, 2340.

(67) Busnengo, H. F.; Salin, A.; Dong, W. *J. Chem. Phys.* **2000**, *112*, 7641.
(68) Diaz, C.; Olsen, R. A.; Busnengo, H. F.; Kroes, G. J. *J. Phys. Chem. C* **2010**, *114*, 11192.
(69) Ischtwan, J.; Collins, M. A. *J. Chem. Phys.* **1994**, *100*, 8080.
(70) Collins, M. A. *Theo. Chem. Acc.* **2002**, *108*, 313.
(71) Crespos, C.; Collins, M. A.; Pijper, E.; Kroes, G.-J. *J. Chem. Phys.* **2004**, *120*, 2392.
(72) Abufager, P. N.; Crespos, C.; Busnengo, H. F. *Phys. Chem. Chem. Phys.* **2007**, *9*, 2258.
(73) Frankcombe, T. J.; Collins, M. A.; Zhang, D. H. *J. Chem. Phys.* **2012**, *137*, 144701.
(74) Braams, B. J.; Bowman, J. M. *Int. Rev. Phys. Chem.* **2009**, *28*, 577.
(75) Bowman, J. M.; Czakó, G.; Fu, B. *Phys. Chem. Chem. Phys.* **2011**, *13*, 8094.
(76) Xie, Z.; Bowman, J. M. *J. Chem. Theo. Comp.* **2010**, *6*, 26.
(77) Jiang, B.; Ren, X.; Xie, D.; Guo, H. *Proc. Natl. Acad. Sci. USA* **2012**, *109*, 10224.
(78) Jiang, B.; Liu, R.; Li, J.; Xie, D.; Yang, M.; Guo, H. *Chem. Sci.* **2013**, *4*, 3249.
(79) Handley, C. M.; Popelier, P. L. A. *J. Phys. Chem. A* **2010**, *114*, 3371.
(80) Behler, J. *Phys. Chem. Chem. Phys.* **2011**, *13*, 17930.
(81) Raff, L. M.; Komanduri, R.; Hagan, M.; Bukkapatnam, S. T. S. *Neural Networks in Chemical Reaction Dynamics*; Oxford University Press: Oxford, 2012.
(82) Lorenz, S.; Groß, A.; Scheffler, M. *Chem. Phys. Lett.* **2004**, *395*, 210.
(83) Lorenz, S.; Scheffler, M.; Gross, A. *Phys. Rev. B* **2006**, *73*, 115431.
(84) Behler, J.; Lorenz, S.; Reuter, K. *J. Chem. Phys.* **2007**, *127*, 014705.
(85) Ludwig, J.; Vlachos, D. G. *J. Chem. Phys.* **2007**, *127*, 154716.
(86) Manzhos, S.; Yamashita, K. *Surf. Sci.* **2010**, *604*, 555.
(87) Liu, T.; Fu, B.; Zhang, D. H. *Sci. China: Chem.* **2014**, *57*, 147.
(88) Jiang, B.; Guo, H. *J. Chem. Phys.* **2014**, *141*, 034109.
(89) Jiang, B.; Guo, H. *J. Chem. Phys.* **2013**, *139*, 054112.
(90) Li, J.; Jiang, B.; Guo, H. *J. Chem. Phys.* **2013**, *139*, 204103.
(91) Li, J.; Chen, J.; Zhang, D. H.; Guo, H. *J. Chem. Phys.* **2014**, *140*, 044327.
(92) Li, J.; Guo, H. *Phys. Chem. Chem. Phys.* **2014**, *16*, 6753.
(93) Li, A.; Guo, H. *J. Chem. Phys.* **2014**, *140*, 224313.
(94) Li, J.; Chen, J.; Zhao, Z.; Xie, D.; Zhang, D. H.; Guo, H. *J. Chem. Phys.* **2015**, *142*, 204302.
(95) Goikoetxea, I.; Beltran, J.; Meyer, J.; Juaristi, J. I.; Alducin, M.; Reuter, K. *New J. Phys.* **2012**, *14*, 013050.
(96) Jiang, B.; Guo, H. *Phys. Rev. Lett.* **2015**, *114*, 166101.
(97) Blöchl, P. E. *Phys. Rev. B* **1994**, *50*, 17953.
(98) Monkhorst, H. J.; Pack, J. D. *Phys. Rev. B* **1976**, *13*, 5188.
(99) Perdew, J. P.; Burke, K.; Ernzerhof, M. *Phys. Rev. Lett.* **1996**, *77*, 3865.
(100) Perdew, J. P. *Phys. Rev. B* **1986**, *33*, 8822.
(101) Methfessel, M.; Paxton, A. T. *Phys. Rev. B* **1989**, *40*, 3616.
(102) Kresse, G.; Furthmuller, J. *Phys. Rev. B* **1996**, *54*, 11169.
(103) Kresse, G.; Furthmuller, J. *Comp. Mater. Sci.* **1996**, *6*, 15.
(104) Libisch, F.; Huang, C.; Carter, E. A. *Acc. Chem. Res.* **2014**, *47*, 2768.
(105) Tully, J. C. *Annu. Rev. Phys. Chem.* **1980**, *31*, 319.
(106) Gerber, R. B. *Chem. Rev.* **1987**, *87*, 29.
(107) Hase, W. L. In *Encyclopedia of Computational Chemistry*; Alinger, N. L., Ed.; Wiley: New York, 1998; Vol. 1.
(108) Hu, X.; Hase, W. L.; Pirraglia, T. *J. Comp. Chem.* **1991**, *12*, 1014.

(109) Harris, J.; Simon, J.; Luntz, A. C.; Mullins, C. B.; Rettner, C. T. *Phys. Rev. Lett.* **1991**, *67*, 652.
(110) Luntz, A. C.; Harris, J. *Surf. Sci.* **1991**, *258*, 397.
(111) Jansen, A. P. J.; Burghgraef, H. *Surf. Sci.* **1995**, *344*, 149.
(112) Carre, M.-N.; Jackson, B. *J. Chem. Phys.* **1998**, *108*, 3722.
(113) Halonen, L.; Bernasek, S. L.; Nesbitt, D. J. *J. Chem. Phys.* **2001**, *115*, 5611.
(114) Xiang, Y.; Zhang, J. Z. H.; Wang, D. Y. *J. Chem. Phys.* **2002**, *117*, 7698.
(115) Nave, S.; Jackson, B. *Phys. Rev. Lett.* **2007**, *98*, 173003.
(116) Nave, S.; Jackson, B. *J. Chem. Phys.* **2007**, *127*, 224702.
(117) Nave, S.; Jackson, B. *J. Chem. Phys.* **2009**, *130*, 054701.
(118) Tiwari, A. K.; Nave, S.; Jackson, B. *Phys. Rev. Lett.* **2009**, *103*, 253201.
(119) Tiwari, A. K.; Nave, S.; Jackson, B. *J. Chem. Phys.* **2010**, *132*, 134702.
(120) Krishnamohan, G. P.; Olsen, R. A.; Kroes, G.-J.; Gatti, F.; Woittequand, S. *J. Chem. Phys.* **2010**, *133*, 144308.
(121) Jiang, B.; Xie, D.; Guo, H. *Chem. Sci.* **2013**, *4*, 503.
(122) Jiang, B.; Li, J.; Xie, D.; Guo, H. *J. Chem. Phys.* **2013**, *138*, 044704.
(123) Light, J. C.; Carrington Jr., T. *Adv. Chem. Phys.* **2000**, *114*, 263.
(124) Zare, R. N. *Angular Momentum*; Wiley: New York, 1988.
(125) Mandelshtam, V. A.; Taylor, H. S. *J. Chem. Phys.* **1995**, *102*, 7390.
(126) Chen, R.; Guo, H. *J. Chem. Phys.* **1996**, *105*, 3569.
(127) Gray, S. K.; Balint-Kurti, G. G. *J. Chem. Phys.* **1998**, *108*, 950.
(128) Lin, S. Y.; Guo, H. *J. Chem. Phys.* **2003**, *119*, 11602.
(129) Manthe, U. *Mole. Phys.* **2011**, *109*, 1415.
(130) Palma, J.; Clary, D. C. *J. Chem. Phys.* **2000**, *112*, 1859.
(131) Yang, M.; Zhang, D. H.; Lee, S.-Y. *J. Chem. Phys.* **2002**, *117*, 9539.
(132) Liu, R.; Xiong, H.; Yang, M. *J. Chem. Phys.* **2012**, *137*, 174113.
(133) Zhang, W.; Zhou, Y.; Wu, G.; Lu, Y.; Pan, H.; Fu, B.; Shuai, Q.; Liu, L.; Liu, S.; Zhang, L.; Jiang, B.; Dai, D.; Lee, S.-Y.; Xie, Z.; Braams, B. J.; Bowman, J. M.; Collins, M. A.; Zhang, D. H.; Yang, X. *Proc. Natl. Acad. Sci. USA* **2010**, *107*, 12782.
(134) Zhang, Z.; Zhou, Y.; Zhang, D. H.; Czakó, G.; Bowman, J. M. *J. Phys. Chem. Lett.* **2012**, *3*, 3416.
(135) Liu, R.; Yang, M.; Czakó, G.; Bowman, J. M.; Li, J.; Guo, H. *J. Phys. Chem. Lett.* **2012**, *3*, 3776.
(136) Navin, J. K.; Donald, S. B.; Tinney, D. G.; Cushing, G. W.; Harrison, I. *J. Chem. Phys.* **2012**, *136*, 061101.
(137) Jackson, B.; Nave, S. *J. Chem. Phys.* **2011**, *135*, 114701.
(138) Killelea, D. R.; Utz, A. L. *Phys. Chem. Chem. Phys.* **2013**, *15*, 20545.
(139) Polanyi, J. C. *Science* **1987**, *236*, 680.
(140) Li, J.; Guo, H. *J. Phys. Chem. A* **2014**, *118*, 2419.
(141) Jiang, B.; Guo, H. *J. Phys. Chem. C* **2014**, *118*, 26851.
(142) Gokhale, A. A.; Dumesic, J. A.; Mavrikakis, M. *J. Am. Chem. Soc.* **2008**, *130*, 1402.
(143) Grabow, L. C.; Gokhale, A. A.; Evans, S. T.; Dumesic, J. A.; Mavrikakis, M. *J. Phys. Chem. C* **2008**, *112*, 4608.
(144) Phatak, A. A.; Delgass, W. N.; Ribeiro, F. H.; Schneider, W. F. *J. Phys. Chem. C* **2009**, *113*, 7269.
(145) Seenivasan, H.; Tiwari, A. K. *J. Chem. Phys.* **2013**, *139*, 174707.

(146) Seenivasan, H.; Tiwari, A. K. *J. Chem. Phys.* **2014**, *140*, 174704.
(147) Henderson, M. A. *Surf. Sci. Rep.* **2002**, *46*, 1.
(148) Laffir, F. R.; Fiorin, V.; King, D. A. *J. Chem. Phys.* **2008**, *128*, 114717.
(149) Mondal, A.; Seenivasan, H.; Tiwari, A. K. *J. Chem. Phys.* **2012**, *137*, 094708.
(150) Sinha, A.; Hsiao, M. C.; Crim, F. F. *J. Chem. Phys.* **1991**, *94*, 4928.
(151) Sinha, A.; Thoemke, J. D.; Crim, F. F. *J. Chem. Phys.* **1992**, *96*, 372.
(152) Thoemke, J. D.; Pfeiffer, J. M.; Metz, R. B.; Crim, F. F. *J. Phys. Chem.* **1995**, *99*, 13748.
(153) Bronikowski, M. J.; Simpson, W. R.; Zare, R. N. *J. Phys. Chem.* **1993**, *97*, 2194.
(154) Bronikowski, M. J.; Simpson, W. R.; Zare, R. N. *J. Phys. Chem.* **1993**, *97*, 2204.
(155) Kudla, K.; Schatz, G. C. *Chem. Phys. Lett.* **1992**, *193*, 507.
(156) Zhang, D. H.; Light, J. C. *J. Chem. Soc. Faraday Trans.* **1997**, *93*, 691.
(157) Zhang, D. H.; Collins, M. A.; Lee, S.-Y. *Science* **2000**, *290*, 961.
(158) Fu, B.; Zhang, D. H. *J. Chem. Phys.* **2013**, *138*, 184308.
(159) Fu, B.; Zhang, D. H. *J. Chem. Phys.* **2015**, *142*, 064314.
(160) Jiang, B.; Xie, D.; Guo, H. *J. Chem. Phys.* **2011**, *135*, 084112.
(161) Li, J.; Song, H.; Guo, H. *Phys. Chem. Chem. Phys.* **2015**, *17*, 4259.
(162) Díaz, C.; Pijper, E.; Olsen, R. A.; Busnengo, H. F.; Auerbach, D. J.; Kroes, G.-J. *Science* **2009**, *326*, 832.
(163) Rettner, C. T.; Pfnur, H. E.; Auerbach, D. J. *Phys. Rev. Lett.* **1985**, *54*, 2716.
(164) Lee, M. B.; Yang, Q. Y.; Ceyer, S. T. *J. Chem. Phys.* **1987**, *87*, 2724.
(165) Luntz, A. C.; Bethune, D. S. *J. Chem. Phys.* **1989**, *90*, 1274.
(166) McMaster, M. C.; Madix, R. J. *J. Chem. Phys.* **1993**, *98*, 9963.
(167) Holmblad, P. M.; Wambach, J.; Chorkendorff, I. *J. Chem. Phys.* **1995**, *102*, 8255.
(168) Walker, A. V.; King, D. A. *Phys. Rev. Lett.* **1999**, *82*, 5156.
(169) Rettner, C. T.; Pfnür, H. E.; Auerbach, D. J. *J. Chem. Phys.* **1986**, *84*, 4163.
(170) Kratzer, P.; Hammer, B.; Nørskov, J. K. *J. Chem. Phys.* **1996**, *105*, 5595.
(171) Abild-Pedersen, F.; Lytken, O.; Engbæk, J.; Nielsen, G.; Chorkendorff, I.; Nørskov, J. K. *Surf. Sci.* **2005**, *590*, 127.
(172) Liu, Z.-P.; Hu, P. *J. Am. Chem. Soc.* **2003**, *125*, 1958.
(173) Anghel, A. T.; Wales, D. J.; Jenkins, S. J.; King, D. A. *Phys. Rev. B* **2005**, *71*, 113410.
(174) Henkelman, G.; Arnaldsson, A.; Jónsson, H. *J. Chem. Phys.* **2006**, *124*, 044706.
(175) Nave, S.; Tiwari, A. K.; Jackson, B. *J. Chem. Phys.* **2010**, *132*, 054705.
(176) Milot, R.; Jansen, A. P. J. *Phys. Rev. B* **2000**, *61*, 15657.
(177) Xiang, Y.; Zhang, J. Z. H. *J. Chem. Phys.* **2003**, *118*, 8954.
(178) Nave, S.; Jackson, B. *Phys. Rev. B* **2010**, *81*, 233408.
(179) Jackson, B.; Nave, S. *J. Chem. Phys.* **2013**, *138*, 174705.
(180) Miller, W. H.; Handy, N. C.; Adams, J. E. *J. Chem. Phys.* **1980**, *72*, 99.
(181) Krishnamohan, G. P.; Olsen, R. A.; Valdes, A.; Kroes, G.-J. *Phys. Chem. Chem. Phys.* **2010**, *12*, 7654.
(182) Mastromatteo, M.; Jackson, B. *J. Chem. Phys.* **2013**, *139*, 194701.
(183) Han, D.; Nave, S.; Jackson, B. *J. Phys. Chem. A* **2013**, *117*, 8651.
(184) Guo, H.; Jackson, B. *J. Phys. Chem. C* **2015**, *in press, DOI: 10.1021/acs.jpcc.5b00915*.
(185) Shen, X. J.; Lozano, A.; Dong, W.; Busnengo, H. F.; Yan, X. H. *Phys. Rev. Lett.* **2014**, *112*, 046101.
(186) Jiang, B.; Guo, H. *J. Phys. Chem. C* **2013**, *117*, 16127.
(187) Jiang, B.; Guo, H. *J. Chin. Chem. Soc.* **2014**, *61*, 841.

(188) Simpson, W. R.; Rakitzis, T. P.; Kandel, S. A.; Orr-Ewing, A. J.; Zare, R. N. *J. Chem. Phys.* **1995**, *103*, 7313.
(189) Kim, Z. H.; Bechtel, H. A.; Zare, R. N. *J. Am. Chem. Soc.* **2001**, *123*, 12714.
(190) Bechtel, H. A.; Kim, Z.-H.; Camden, J. P.; Zare, R. N. *J. Chem. Phys.* **2004**, *120*, 791.
(191) Bechtel, H. A.; Camden, J. P.; Brown, D. J. A.; Zare, R. N. *J. Chem. Phys.* **2004**, *120*, 5096.
(192) Camden, J. P.; Bechtel, H. A.; Brown, D. J. A.; Zare, R. N. *J. Chem. Phys.* **2005**, *123*, 134301.
(193) Yoon, S.; Henton, S.; Zivkovic, A. N.; Crim, F. F. *J. Chem. Phys.* **2002**, *116*, 10744.
(194) Yoon, S.; Holiday, R. J.; Crim, F. F. *J. Chem. Phys.* **2003**, *119*, 4755.
(195) Yoon, S.; Holiday, R. J.; Sibert III, E. L.; Crim, F. F. *J. Chem. Phys.* **2003**, *119*, 9568.
(196) Holiday, R. J.; Kwon, C. H.; Annesley, C. J.; Crim, F. F. *J. Chem. Phys* **2006**, *125*, 133101.
(197) Ukraintsev, V. A.; Harrison, I. *J. Chem. Phys.* **1992**, *96*, 6307.
(198) Bukoski, A.; Harrison, I. *J. Chem. Phys.* **2003**, *118*, 843.
(199) Abbott, H. L.; Bukoski, A.; Harrison, I. *J. Chem. Phys.* **2004**, *121*, 3792.
(200) Li, J.; Jiang, B.; Guo, H. *J. Am. Chem. Soc.* **2013**, *135*, 982.
(201) Song, H.; Guo, H. *J. Phys. Chem. A* **2015**, *119*, 826.
(202) Dai, J.; Light, J. C. *J. Chem. Phys.* **1997**, *107*, 1676.
(203) Liu, T.; Fu, B.; Zhang, D. H. *J. Chem. Phys.* **2014**, *141*, 194302.
(204) Ramos, M.; Batista, M. N.; Martínez, A. E.; Busnengo, H. F. In *Dynamics of Gas-Surface Interactions*; Muino, R. D., Busnengo, H. F., Eds.; Springer: Heidelberg, 2013.
(205) Seets, D. C.; Reeves, C. T.; Ferguson, B. A.; Wheeler, M. C.; Mullins, C. B. *J. Chem. Phys* **1997**, *107*, 10229.
(206) Dombrowski, E.; Peterson, E.; Del Sesto, D.; Utz, A. L. *Catal. Today* **2015**, *244*, 10.

Figure captions:

Figure 1. Measured initial sticking probabilities on Ni(100) for the ground and excited vibrational levels of methane as a function of translational energy at a surface temperature of 475 K. Open symbols correspond to laser-off data from Juurlink et al. (black circles)[26] and Schmid et al. (red squares).[30] Solid symbols correspond to excited state reaction probabilities ($v_3 = 1$) (black circles),[32] ($v_3 = 2$) (red squares),[30] and ($v_1 = 1$) (green diamonds).[34] Adapted from Ref. 9 with permission.

Figure 2. Definition of the coordinates used in studying DC of water (a) and methane (b) on Ni(111).

Figure 3. Contour plots of the PESs and transition state geometries for the DC of water (upper panel) and methane (lower panel) on Ni(111). The definition of the reactive coordinates are given in Figure 2, while all other coordinates are relaxed. The contour interval is 10 kJ/mol.

Figure 4. Dependence of the DC reactivity of H_2O on Cu(111) on low rotational excitations ($J_{K_aK_c}$) (a) and orientations (*M*) (b). These reaction probabilities were obtained from 6D QD calculations without corrections on impact sites and lattice effects. Adapted from Ref. 122 with permission.

Figure 5. Alignment of reactant normal mode vectors with the reaction coordinate vector at the transition state for the DC of H_2O, D_2O, and HOD on Ni(111) (upper four panels) and CH_4, CHD_3, and CH_2D_2 on Ni(111) (lower six panels).

Figure 6. Comparison of calculated and measured initial sticking probabilities for D_2O on Ni(111). The filled points represent the experimental data and the dotted lines are fitted S-shape

reactivity curves. Solid lines are the results of quantum dynamics calculations on the 6D scaled PES and the black stars are calculated laser-off reactivities including the thermal vibrational excitation for the nozzle temperature used in each experiment. Adapted from Ref. 48 with permission.

Figure 7. QCT dissociation probabilities of $D_2O(v_1, v_2, v_3)$ in normal incidence on the 9D and 6D PESs as a function of translational energy (upper panel) and total energy (lower panel). v_1, v_2, and v_3 denote the symmetric stretching, bending, and asymmetric stretching modes of D_2O, respectively. The total energy is relative to the asymptotic potential plus the zero-point energy of D_2O. Adapted from Ref. 96 with permission.

Figure 8. (a) Fixed-site barrier height (in eV) map in the smallest symmetry irreducible triangle within the approximate C_{6v} symmetry. (b-d) Fixed-site contour plots of the PES as a function of the vertical distance of H_2O COM (z_0) and the distance between the dissociating H atom and COM of the molecule (r), with other coordinates fully relaxed. The saddle point geometries are inserted in the right upper corner. Adapted from Ref. 96 with permission.

Figure 9. Dissociation probabilities of D_2O with nozzle temperatures at 573K (E_t=13.94 kcal/mol), 673K (E_t=15.68 kcal/mol), and 773K (E_t=17.71 kcal/mol), as a function of the incident angle θ, with the total translational energy fixed (upper panel) and the normal component of translational energy fixed (lower panel). Adapted from Ref. 96 with permission.

Figure 10. Upper panel: comparison of measured initial sticking probabilities of the ground and vibrationally excited states of CH_4 on Ni(100) at 475K with those calculated using the RPH approach.[55] RPH probabilities are for the ground (black), $1v_3$ (red), $2v_3$ (green), or $1v_1$ (blue) vibrational state, treating rotational motion in either the adiabatic (solid) or sudden (dashed) limit.

The symbols are experimental data from the groups of Utz (A) and Beck (R). Lower panel: Single-site RPH dissociation probabilities for CH_4 initially excited to antisymmetric stretch (1′ (red) and 1″ (brown)) and symmetric stretch (3′ (blue)) states on Ni(100) with the vibrational non-adiabatic coupling completely switched off (solid symbols), partially switched off (only curvature terms retained, open symbols) and on (solid curves).[137] Adapted from Refs. 55 and 137 with permission.

Figure 11. Comparison of the measured initial sticking probabilities for CH_4 on Ni(111) and those calculated using a 8D QD model on the 12D PES. Adapted from Ref. 78 with permission.

Table I. Experimental and selected theoretical vibrational efficacies for methane dissociative chemisorption on various transition metal surfaces. Estimates from experiments are based on the assumption that initial sticking coefficients for the laser-off condition and excited states have the same shape.

State	E_{vib} (kJ/mol)	Surface	η_{vib}	
			Expt.	Theo.
v_3	36	Ni(100)	0.94 [a, 26]	0.80 [178]
$2v_3$	71	Ni(100)	0.8±0.1 [30]	
v_1	35	Ni(100)	1.4 [a, 34]	0.93 [178]
$3v_4$	45	Ni(100)	⩽0.5 [a, 33]	0.71 [b, 178]
v_3	36	Ni(111)	1.25 [32]	1.15~1.26 [78]
$2v_3$	71	Ni(111)	0.90 [35]	0.90~0.94 [78]
$3v_4$	45	Ni(111)	0.72 [33]	0.59~0.64 [78]
v_2+v_4	34	Ni(111)	0.44 [43]	
v_3	36	Pt(111)	0.7 [44]	
$2v_3$	71	Pt(111)	0.4 [35]	
v_1+v_4	51	Pt(110)-(1×2)	0.67±0.02 [38]	
v_3+v_4	52	Pt(110)-(1×2)	0.54±0.02 [38]	
$2v_3$	72	Pt(110)-(1×2)	0.47±0.02 [38]	
$2v_2+v_4$	52	Pt(110)-(1×2)	0.40±0.03 [38]	
v_3	36	Ir(111)	0.43 [206]	

[a] The shape of the excited state sticking curve is not fully determined, so is the vibrational efficacy.
[b] The theoretical efficacy is for v_4, rather than for $3v_4$ state.

Figure 1.

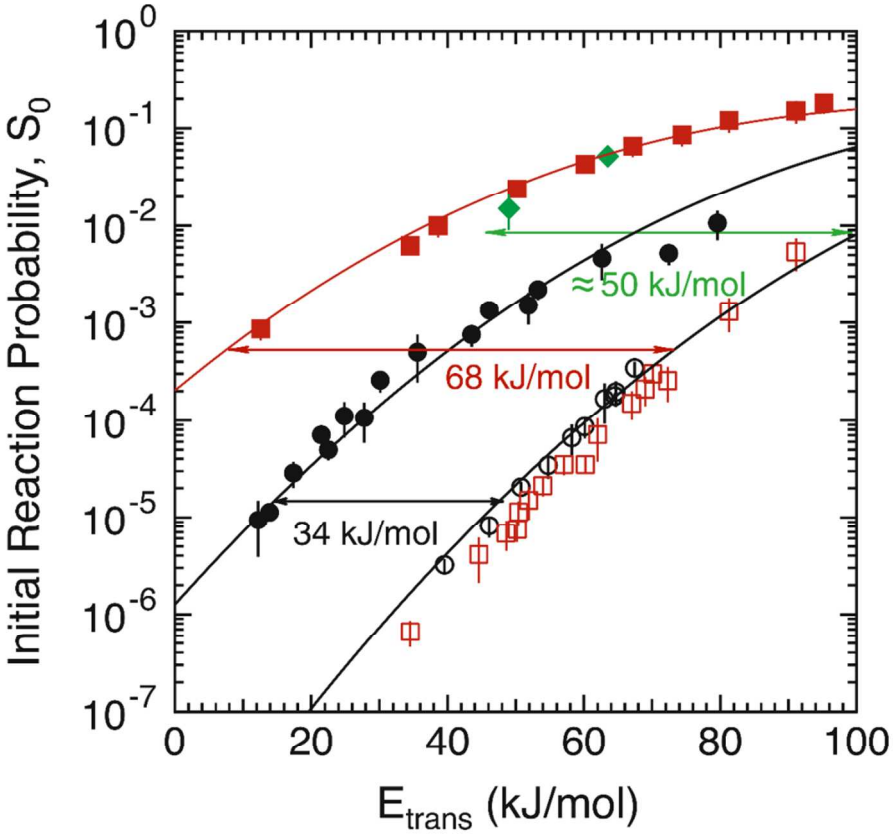
Initial Reaction Probability, S_0
10^0
10^{-1}
10^{-2}
10^{-3}
10^{-4}
10^{-5}
10^{-6}
10^{-7}
0
20
40
60
80
100
E_{trans} (kJ/mol)
≈50 kJ/mol
68 kJ/mol
34 kJ/mol

Figure 2

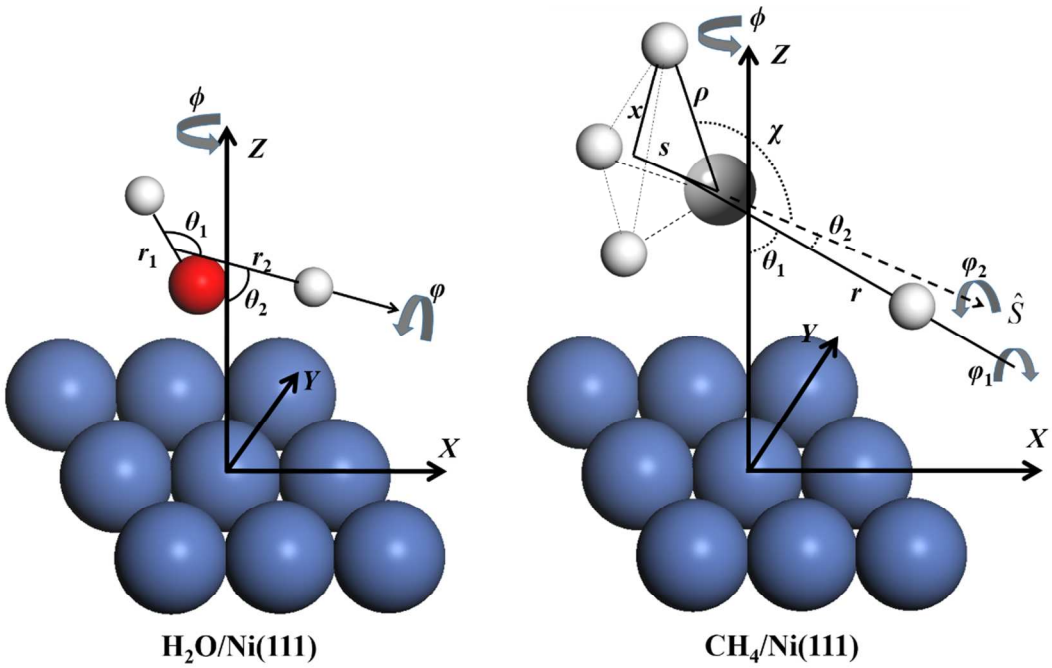

Figure 3

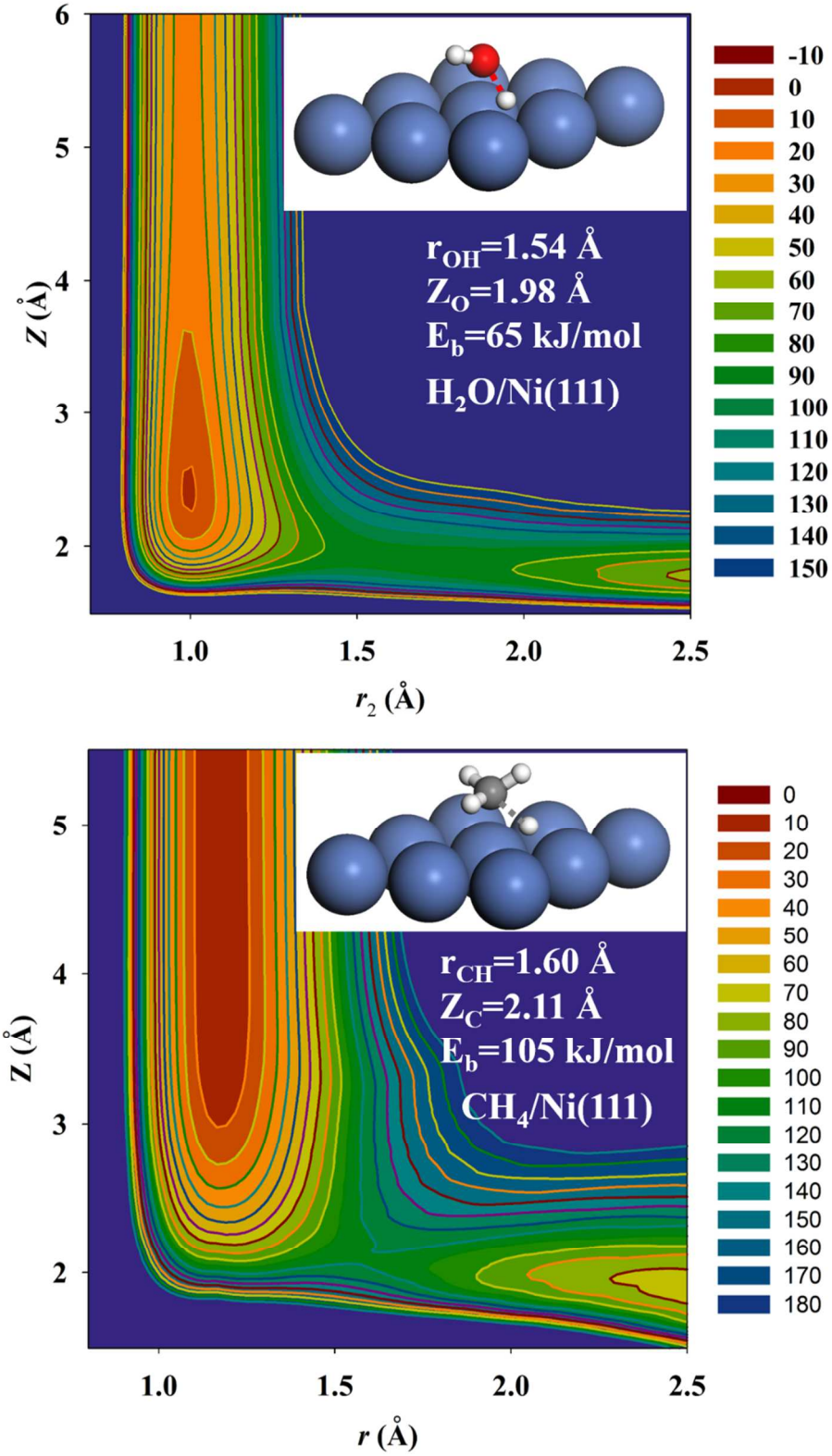
6
5
4
3
2
Z (Å)
1.0
1.5
2.0
2.5
r2 (Å)
rOH=1.54 Å
ZO=1.98 Å
Eb=65 kJ/mol
H2O/Ni(111)
-10
0
10
20
30
40
50
60
70
80
90
100
110
120
130
140
150
5
4
3
2
Z (Å)
1.0
1.5
2.0
2.5
r (Å)
rCH=1.60 Å
ZC=2.11 Å
Eb=105 kJ/mol
CH4/Ni(111)
0
10
20
30
40
50
60
70
80
90
100
110
120
130
140
150
160
170
180

Figure 4

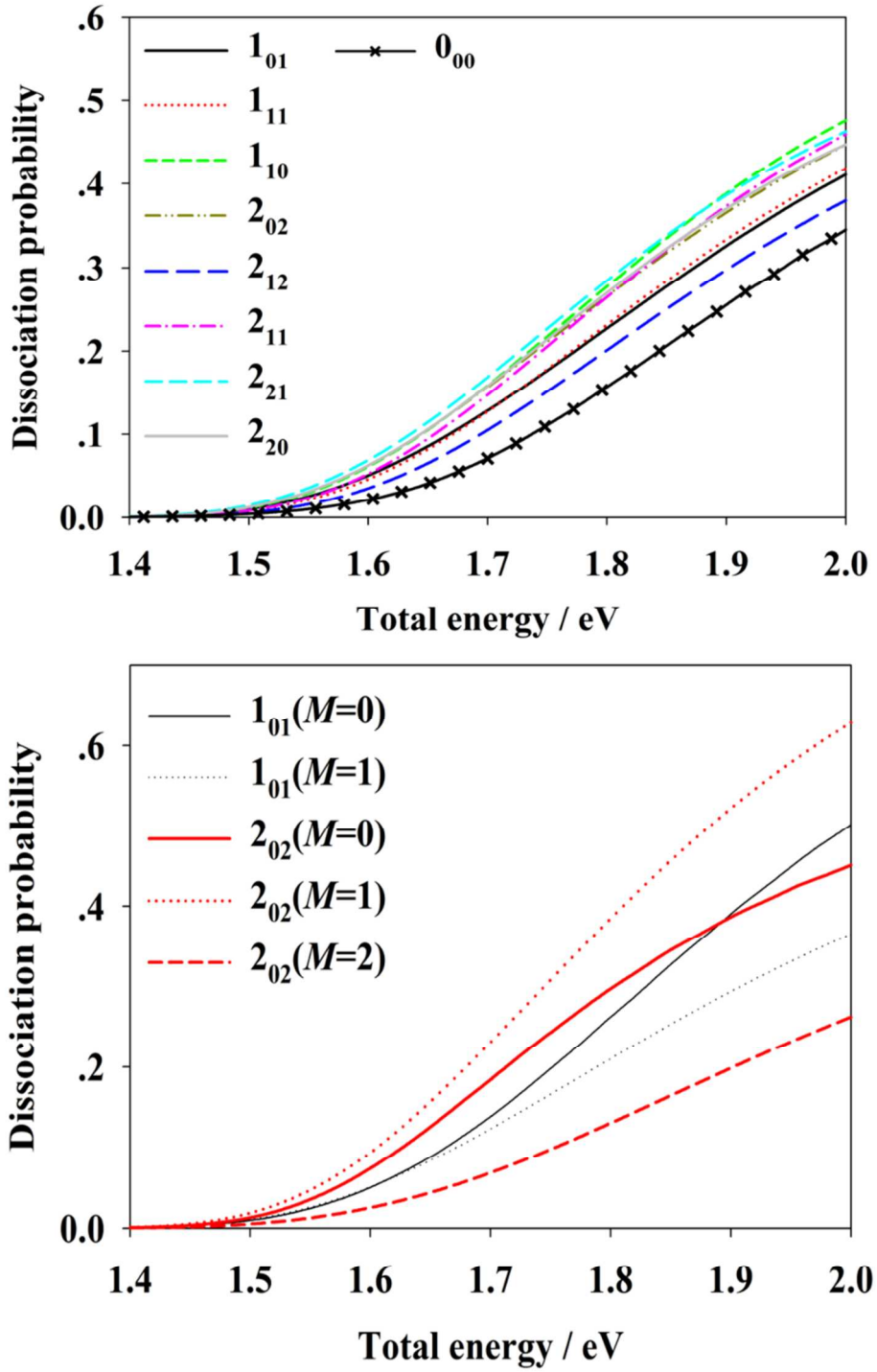
Dissociation probability
Total energy / eV
1.4
1.5
1.6
1.7
1.8
1.9
2.0
0.0
.1
.2
.3
.4
.5
.6
1_{01}
0_{00}
1_{11}
1_{10}
2_{02}
2_{12}
2_{11}
2_{21}
2_{20}
Dissociation probability
Total energy / eV
$1_{01}(M=0)$
$1_{01}(M=1)$
$2_{02}(M=0)$
$2_{02}(M=1)$
$2_{02}(M=2)$

Figure 5

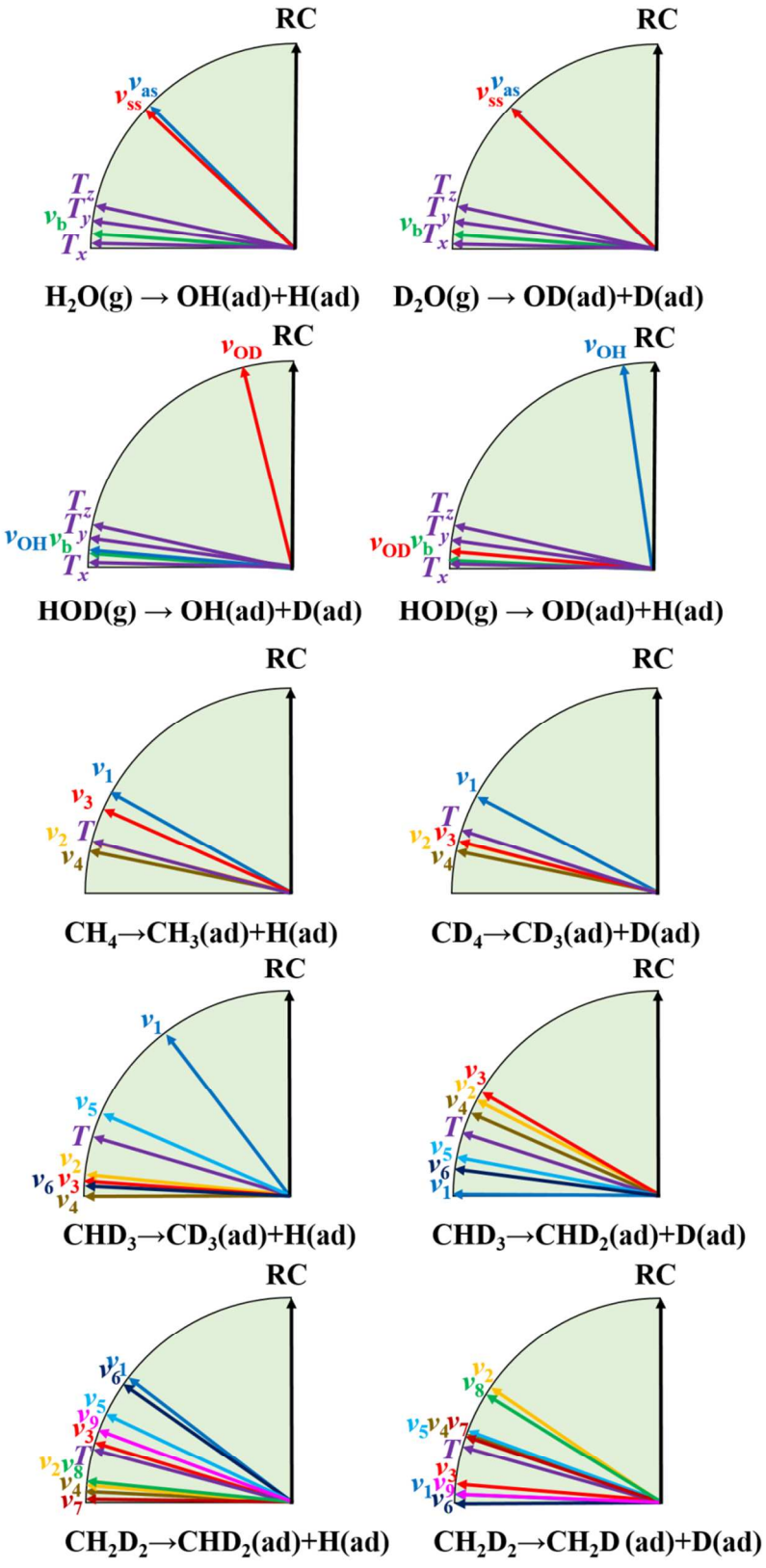
RC
ν_{as}
ν_{ss}
T_z
T_y
ν_b
T_x
$H_2O(g) \rightarrow OH(ad)+H(ad)$
RC
ν_{as}
ν_{ss}
T_z
T_y
ν_b
T_x
$D_2O(g) \rightarrow OD(ad)+D(ad)$
RC
ν_{OD}
T_z
T_y
ν_{OH}
ν_b
T_x
$HOD(g) \rightarrow OH(ad)+D(ad)$
RC
ν_{OH}
T_z
T_y
ν_{OD}
ν_b
T_x
$HOD(g) \rightarrow OD(ad)+H(ad)$
RC
ν_1
ν_3
ν_2
T
ν_4
$CH_4 \rightarrow CH_3(ad)+H(ad)$
RC
ν_1
T
ν_2
ν_3
ν_4
$CD_4 \rightarrow CD_3(ad)+D(ad)$
RC
ν_1
ν_5
T
ν_2
ν_6
ν_3
ν_4
$CHD_3 \rightarrow CD_3(ad)+H(ad)$
RC
ν_3
ν_2
ν_4
T
ν_5
ν_6
ν_1
$CHD_3 \rightarrow CHD_2(ad)+D(ad)$
RC
ν_6
ν_1
ν_5
ν_9
ν_3
T
ν_2
ν_8
ν_4
ν_7
$CH_2D_2 \rightarrow CHD_2(ad)+H(ad)$
RC
ν_2
ν_8
ν_5
ν_4
ν_7
T
ν_1
ν_3
ν_9
ν_6
$CH_2D_2 \rightarrow CH_2D\ (ad)+D(ad)$

Figure 6

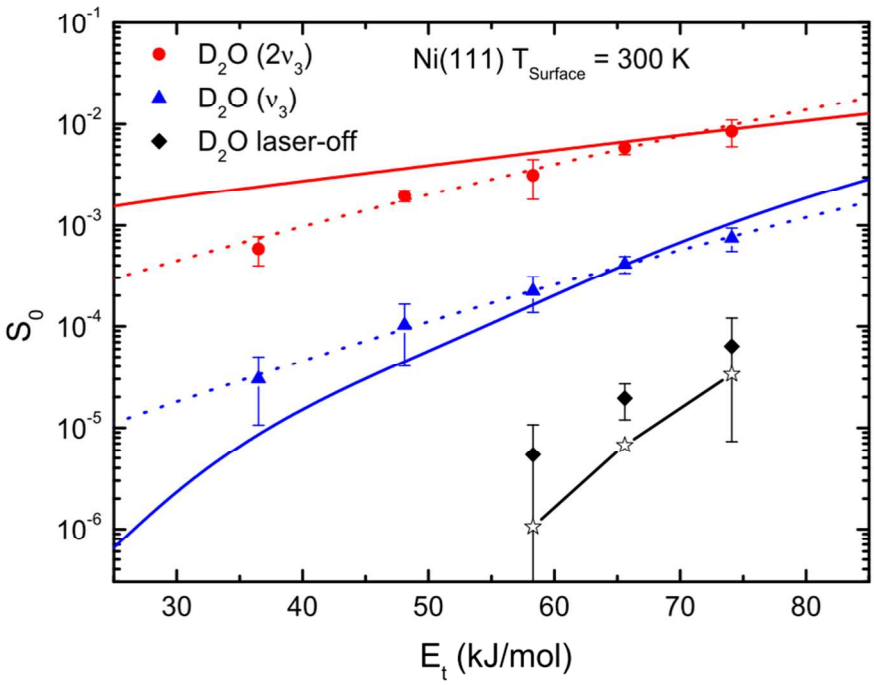
D2O (2ν3)
D2O (ν3)
D2O laser-off
Ni(111) TSurface = 300 K
S0
Et (kJ/mol)
10-1
10-2
10-3
10-4
10-5
10-6
30
40
50
60
70
80

Figure 7

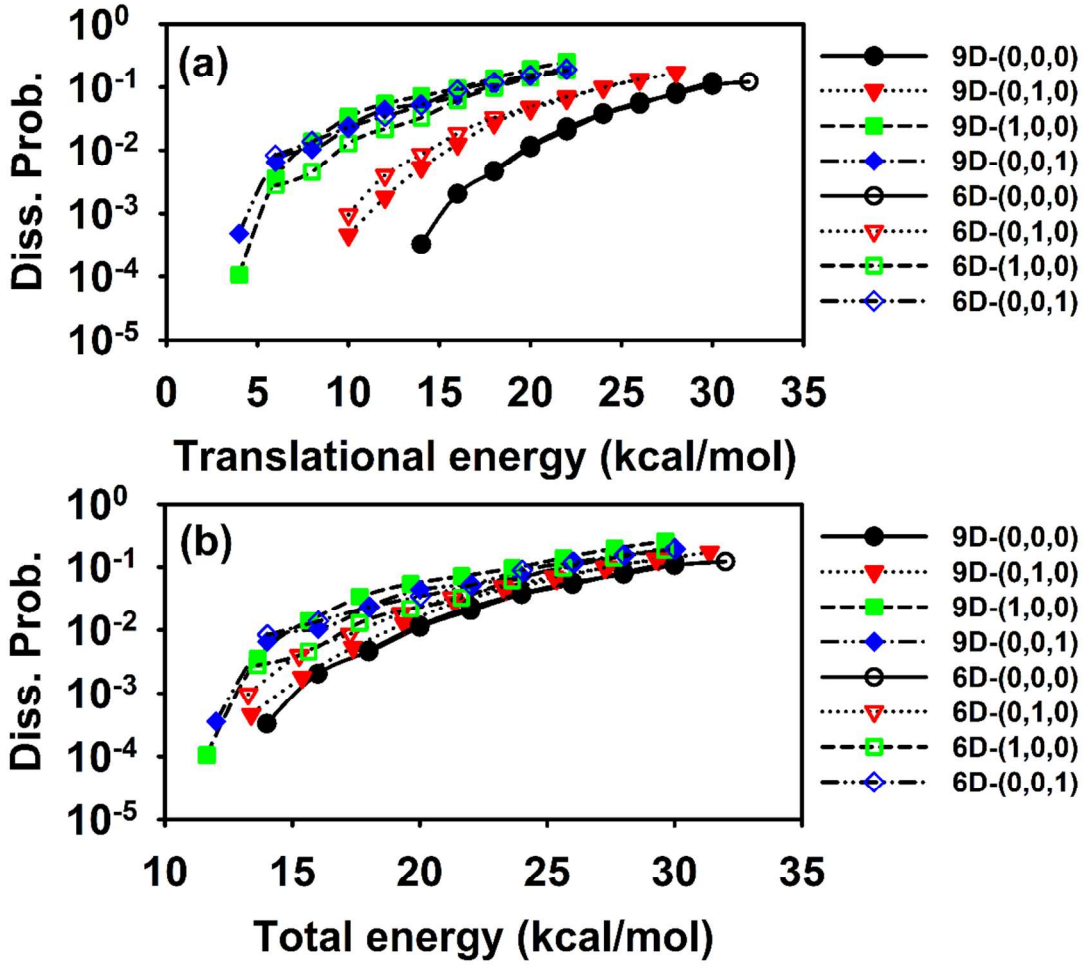
(a)
Diss. Prob.
10^{0}
10^{-1}
10^{-2}
10^{-3}
10^{-4}
10^{-5}
0 5 10 15 20 25 30 35
Translational energy (kcal/mol)
9D-(0,0,0)
9D-(0,1,0)
9D-(1,0,0)
9D-(0,0,1)
6D-(0,0,0)
6D-(0,1,0)
6D-(1,0,0)
6D-(0,0,1)
(b)
Diss. Prob.
10^{0}
10^{-1}
10^{-2}
10^{-3}
10^{-4}
10^{-5}
10 15 20 25 30 35
Total energy (kcal/mol)
9D-(0,0,0)
9D-(0,1,0)
9D-(1,0,0)
9D-(0,0,1)
6D-(0,0,0)
6D-(0,1,0)
6D-(1,0,0)
6D-(0,0,1)

Figure 8

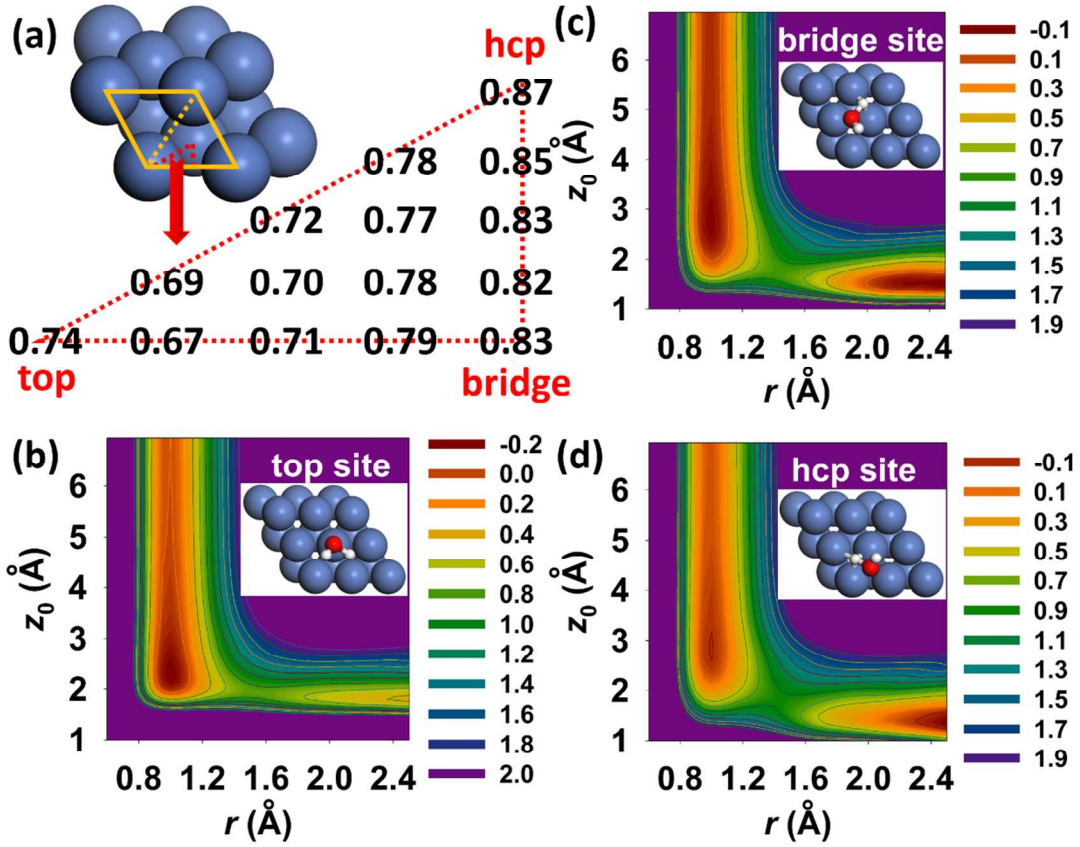
(a)
hcp
top
bridge
0.87
0.78 0.85
0.72 0.77 0.83
0.69 0.70 0.78 0.82
0.74 0.67 0.71 0.79 0.83
(b)
top site
(c)
bridge site
(d)
hcp site
z_0 (Å)
r (Å)
0.8 1.2 1.6 2.0 2.4
-0.2 0.0 0.2 0.4 0.6 0.8 1.0 1.2 1.4 1.6 1.8 2.0
-0.1 0.1 0.3 0.5 0.7 0.9 1.1 1.3 1.5 1.7 1.9

Figure 9

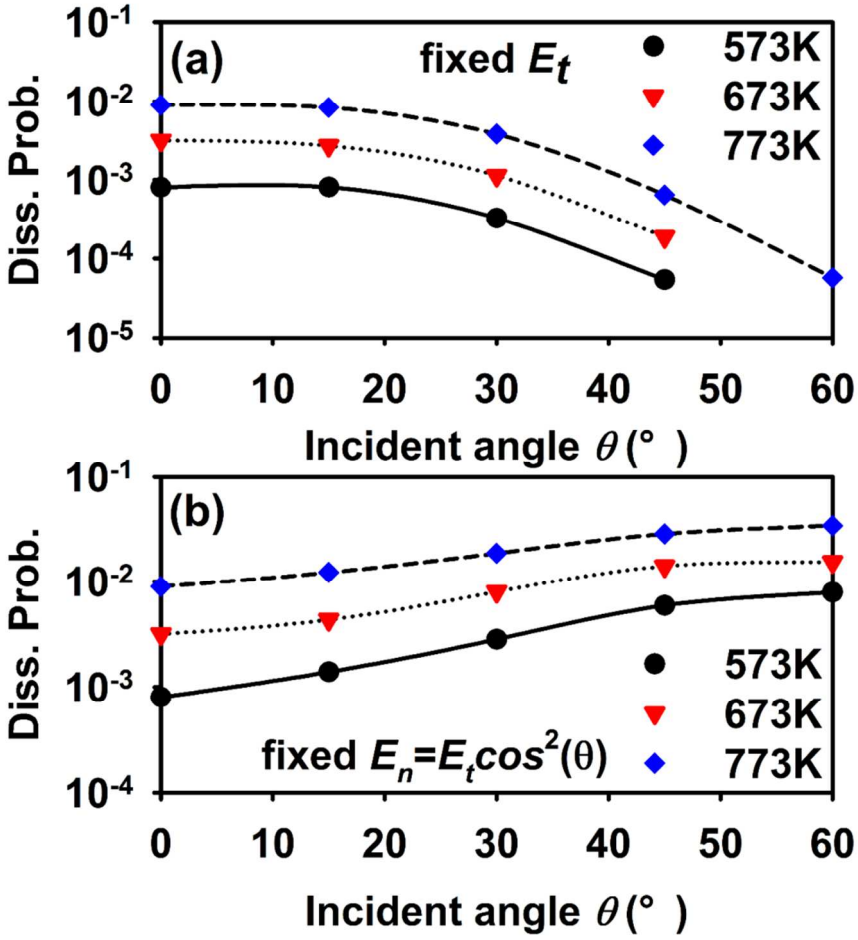
(a)
fixed E_t
573K
673K
773K
Diss. Prob.
10^{-1}
10^{-2}
10^{-3}
10^{-4}
10^{-5}
0 10 20 30 40 50 60
Incident angle θ(°)
(b)
fixed $E_n=E_t\cos^2(\theta)$
573K
673K
773K
Diss. Prob.
10^{-1}
10^{-2}
10^{-3}
10^{-4}
0 10 20 30 40 50 60
Incident angle θ(°)

Figure 10

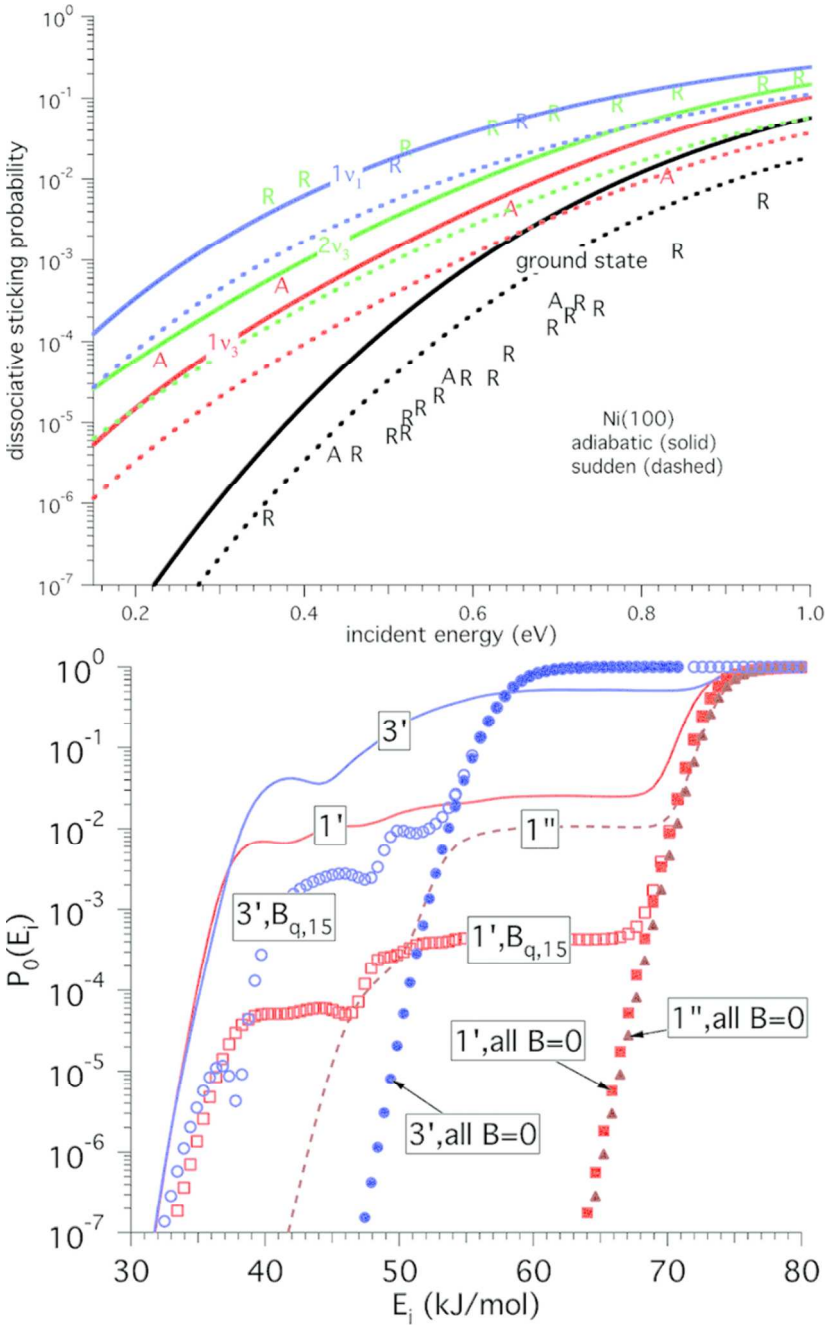
dissociative sticking probability
incident energy (eV)
ground state
Ni(100)
adiabatic (solid)
sudden (dashed)
$1\nu_1$
$2\nu_3$
$1\nu_3$
$P_0(E_i)$
E_i (kJ/mol)
3'
1'
1''
3',$B_{q,15}$
1',$B_{q,15}$
1',all B=0
1'',all B=0
3',all B=0

Figure 11

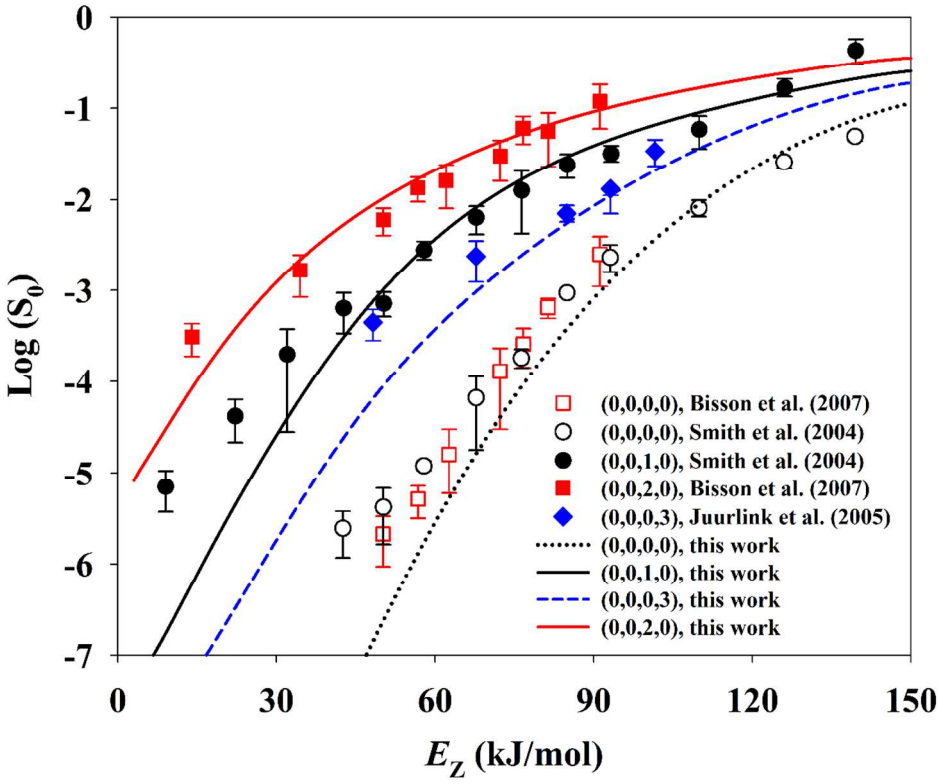
0
-1
-2
-3
-4
-5
-6
-7
Log (S_0)
0
30
60
90
120
150
E_Z (kJ/mol)
(0,0,0,0), Bisson et al. (2007)
(0,0,0,0), Smith et al. (2004)
(0,0,1,0), Smith et al. (2004)
(0,0,2,0), Bisson et al. (2007)
(0,0,0,3), Juurlink et al. (2005)
(0,0,0,0), this work
(0,0,1,0), this work
(0,0,0,3), this work
(0,0,2,0), this work

TOC

Recent advances in quantum dynamical characterization of polyatomic dissociative chemisorption on accurate global potential energy surfaces are critically reviewed.